Available online at www.sciencedirect.com
ScienceDirect
Geochimica et Cosmochimica Acta 72 (2008) 1057–1075
Geochimica et Cosmochimica Acta
www.elsevier.com/locate/gca

Calcium and magnesium isotope systematics in rivers draining the Himalaya-Tibetan-Plateau region: Lithological or fractionation control?

Edward T. Tipper [a,b,*], Albert Galy [a], Mike J. Bickle [a]

[a] Department of Earth Sciences, University of Cambridge, Downing Street, Cambridge, CB2 3EQ, UK
[b] Laboratoire de Géochimie–Cosmochimie, Institut de Physique du Globe de Paris-Université Paris 7, 4 Place Jussieu 75252 Paris cedex 05, France

Received 21 November 2006; accepted in revised form 27 November 2007; available online 25 January 2008

Abstract

In rivers draining the Himalaya-Tibetan-Plateau region, the $^{26}Mg/^{24}Mg$ ratio has a range of 2‰ and the $^{44}Ca/^{42}Ca$ ratio has a range of 0.6‰. The average $\delta^{26}Mg$ values of tributaries from each of the main lithotectonic units (Tethyan Sedimentary Series (TSS), High Himalayan Crystalline Series (HHCS) and Lesser Himalayan Series (LHS)) are within 2 standard deviation analytical uncertainty (0.14‰). The consistency of average riverine $\delta^{26}Mg$ values is in contrast to the main rock types (limestone, dolostone and silicate) which range in their average $\delta^{26}Mg$ values by more than 2‰. Tributaries draining the dolostones of the LHS differ in their $\delta^{44}_{42}Ca$ values compared to tributaries from the TSS and HHCS. The chemistry of these river waters is strongly influenced by dolostone (solute Mg/Ca close to unity) and both $\delta^{26}Mg$ (−1.31‰) and $\delta^{44}_{42}Ca$ (0.64‰) values are within analytical uncertainty of the LHS dolostone. These are the most elevated $\delta^{44}_{42}Ca$ values in rivers and rock reported so far demonstrating that both riverine and bedrock $\delta^{44}_{42}Ca$ values may show greater variability than previously thought.

Although rivers draining TSS limestone have the lowest $\delta^{26}Mg$ and $\delta^{44}_{42}Ca$ values at −1.41 and 0.42‰, respectively, both are offset to higher values compared to bedrock TSS limestone. The average $\delta^{26}Mg$ value of rivers draining mainly silicate rock of the HHCS is −1.25‰, lower by 0.63‰ than the average silicate rock. These differences are consistent with a fractionation of $\delta^{26}Mg$ values during silicate weathering. Given that the proportion of Mg exported from the Himalaya as solute Mg is small, the difference in $^{26}Mg/^{24}Mg$ ratios between silicate rock and solute Mg reflects the $^{26}Mg/^{24}Mg$ isotopic fractionation factor ($\alpha^{Mg}_{silicate-dissolved}$) between silicate and dissolved Mg during incongruent silicate weathering. The value of $\alpha^{Mg}_{silicate-dissolved}$ of 0.99937 implies that in the TSS, solute Mg is primarily derived from silicate weathering, whereas the source of Ca is overwhelmingly derived from carbonate weathering. The average $\delta^{44}_{42}Ca$ value in HHCS rivers is within uncertainty of silicate rock at 0.39‰. The widespread hot springs of the High Himalaya have an average $\delta^{26}Mg$ value of −0.46‰ and an average $\delta^{44}_{42}Ca$ value of 0.5‰, distinct from riverine values for $\delta^{26}Mg$ but similar to riverine $\delta^{44}_{42}Ca$ values. Although rivers draining each major rock type have $\delta^{44}_{42}Ca$ and $\delta^{26}Mg$ values in part inherited from bedrock, there is no correlation with proxies for carbonate or silicate lithology such as Na/Ca ratios, suggesting that Ca and Mg are in part recycled. However, in spite of the vast contrast in vegetation density between the arid Tibetan Plateau and the tropical Lesser Himalaya, the isotopic fractionation factor for Ca and Mg between solute and rocks are not systematically different suggesting that vegetation may only recycle a small amount of Ca and Mg in these catchments.

The discrepancy between solute and solid Ca and Mg isotope ratios in these rivers from diverse weathering environments highlight our lack of understanding concerning the origin and subsequent path of Ca and Mg, bound as minerals in rock, and released as cations in rivers. The fractionation of Ca and Mg isotope ratios may prove useful for tracing mechanisms of chemical alteration. Ca isotope ratios of solute riverine Ca show a greater variability than previously acknowledged. The variability

* Corresponding author. Present address: Institute of Isotope Geochemistry and Mineral Resources, ETH Zurich, Clausiusstrasse 25, NW, 8052 Zurich, Switzerland.
E-mail address: Tipper@erdw.ethz.ch (E.T. Tipper).

0016-7037/$ - see front matter
doi:10.1016/j.gca.2007.11.029

of Ca isotope ratios in modern rivers will need to be better quantified and accounted for in future models of global Ca cycling, if past variations in oceanic Ca isotope ratios are to be of use in constraining the past carbon cycle.

1. INTRODUCTION

Calcium (Ca) and magnesium (Mg) are the major cations involved in the carbon cycle, and the reaction of atmospheric CO_2 with Ca and Mg from silicate minerals, and subsequent deposition as carbonate in the oceans, have long been thought to provide the feedback which regulates climate over geological time-scales (e.g. Walker et al., 1981; Berner et al., 1983). The ubiquity of Ca and Mg in rocks has however, hampered understanding of riverine chemistry. Quantifying the controls on the weathering feedback, and constraining silicate mineral weathering reactions has proved difficult (e.g. Raymo et al., 1988; West et al., 2005). Among the proxies developed for the quantification of the sources of the alkali-earth elements in the dissolved load of river waters, the isotope ratios of strontium (Sr) have been widely applied but also questioned. The Himalaya-Tibetan-Plateau (HTP) region has received significant attention concerning chemical weathering, because of the potential link between the monotonous increase in marine Sr isotope ratios during the Cenozoic and the uplift and exhumation of the HTP (Richter et al., 1992), which may have increased weathering rates in this region (Raymo et al., 1988). However, the interpretation of Sr isotope ratios as a tracer of silicate weathering in the HTP region has been frustrated by the presence of radiogenic carbonate, with similar Sr isotope ratios to silicate minerals. There is a continuing controversy over the quantification of carbonate and silicate derived Sr during weathering (e.g. Edmond, 1992; Krishnaswami et al., 1992; Palmer and Edmond, 1992; Pande et al., 1994; Quade et al., 1997; Harris et al., 1998; Galy et al., 1999; English et al., 2000; Bickle et al., 2003; Oliver et al., 2003; Bickle et al., 2005).

Proxies for the fractions of cations derived from silicate or carbonate minerals, such as elemental ratios rely on assumptions about the nature of the weathering reactions. For example, in the HTP region, all tracers for quantifying the proportion of carbonate to silicate weathering involving Ca are complicated by the non-conservative behaviour of Ca, with up to 70% of the total Ca initially in solution, reported to be removed from Himalayan rivers by the precipitation of secondary calcite (Galy et al., 1999; Jacobson et al., 2002; Bickle et al., 2005; Tipper et al., 2006a). In this paper, we investigate the behaviour of Ca and Mg in rivers from the HTP by analysis of their isotopic composition. Such data can be obtained by either multi-collector inductively coupled plasma mass spectrometry (MC-ICP-MS) or thermal ionisation mass spectrometry and has already been demonstrated as a powerful new tool for investigating the global cycles of Ca and Mg (e.g. De La Rocha and DePaolo, 2000; Schmitt et al., 2003; Farkaš et al., 2006; Tipper et al., 2006b) and the under-constrained weathering reactions by which these elements are released from the continental crust (e.g. Schmitt et al., 2003; Tipper et al., 2006a).

Stable isotope ratios in rivers are controlled by mixtures of waters with distinct compositions, often inherited from source rock heterogeneity, but also by fractionation during a series of processes associated with weathering reactions. Recent work on Ca and Mg isotope ratios in large rivers has demonstrated that there is a weak dependency on lithology (Schmitt et al., 2003; Tipper et al., 2006b). At a smaller scale, the fractionation of Ca and Mg isotope ratios during weathering reactions, such as the uptake of Ca by vegetation (Schmitt et al., 2003; Wiegand et al., 2005) or the precipitation of Ca and/or Mg bearing minerals in soil (Tipper et al., 2006a), appear to be the dominant factor controlling these isotope ratios. The combined effects of variable sources and fractionation by weathering reactions make the quantification of the origin of solute Ca and Mg surprisingly difficult. In the case of the HTP region, or any other place where the $^{87}Sr/^{86}Sr$ ratio is not a reliable proxy for lithology, the measurement of their isotope ratios may therefore significantly improve our understanding of Ca and Mg in rivers.

In this paper, we present a substantial new set of data of Ca and Mg isotope ratios from the Himalaya-Tibetan-Plateau region, in both large and small rivers allowing the first detailed assessment of the lithological control on solute Ca and Mg isotope ratios and an insight into the roles of vegetation and weathering reactions in modifying riverine Ca and Mg isotope ratios.

2. STUDY AREA

A range of samples of large and small rivers have been analysed, from Nepal, Tibet and Bangladesh in the HTP region (Fig. 1a). The majority of samples however are from the much studied Marsyandi catchment, Nepal Himalaya (Fig. 1b) (Galy et al., 1999; Evans et al., 2001; Bickle et al., 2005; Kisakurek et al., 2005; Tipper et al., 2006a,c).

The Marsyandi catchment is an ideal location to study the systematics of riverine Ca and Mg isotope ratios because of:

(1) the range of rock types drained with published data already existing on their Ca and Mg isotope ratios (Tipper et al., 2006a);
(2) the climatic and vegetation gradient (Fig. 1c) across the catchment and,
(3) the relatively well constrained river chemistry in the basin.

2.1. Main rock types of the Marsyandi basin

Three distinct rock types can be identified in the Marsyandi catchment, principally limestone, silicate and dolostone (Bordet et al., 1971; Le Fort, 1975; Colchen et al.,

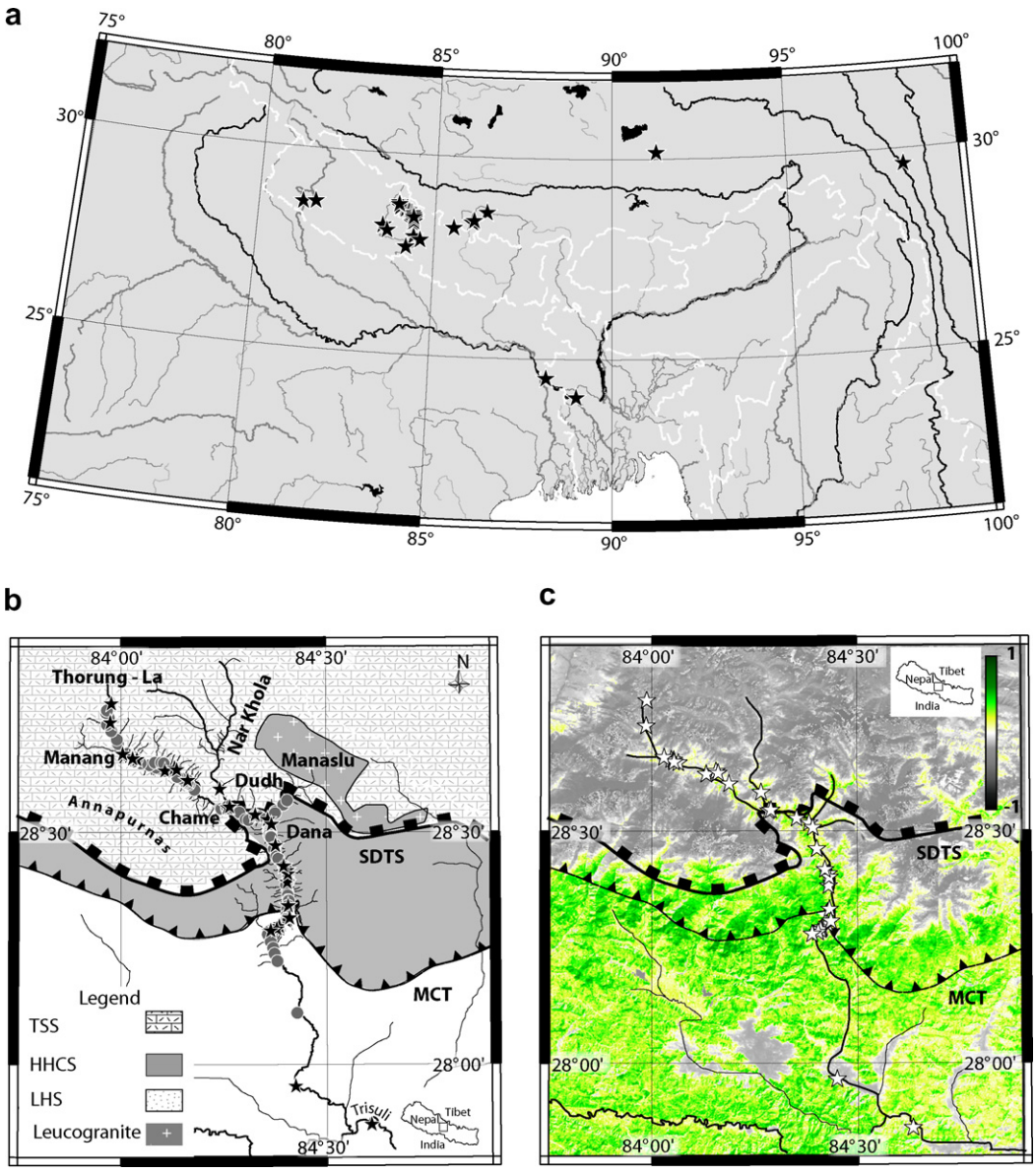

Fig. 1. (a) General location map of samples. Political boundaries shown in white. (b) Geological map of the Marsyandi after Colchen et al. (1986). The main range strikes east–west between the Annapurnas and Manaslu. STDS is the South Tibetan Detachment System and MCT is the Main Central Thrust. (c) Normalised vegetation index (NDVI) of the Marsyandi created by merging Landsat images p141r040, p141r041, p142r040, p142r041 and by combining bands 3 and 4 to calculate the NDVI following Tucker (1979). An NDVI of unity is equivalent to dense vegetation (green). Values less than unity indicate water, ice, bare rock and some cloud cover over the LHS. The stars indicate sampling sites for Ca and Mg isotope ratios, and circles sampling sites which have been analysed for major elements. (For interpretation of the references to colour in this figure legend, the reader is referred to the web version of this article.)

1986) and are representative of the main lithotectonic units found in the Himalaya. Only a summary is provided here (Fig. 1b).

The headwaters of the Marsyandi and its tributaries drain a 50 km transect of variably metamorphosed limestones and siliclastic rocks (Bordet et al., 1971; Schneider and Masch, 1993) known as the Tethyan Sedimentary Series (TSS). These limestones are impure, and pyritic black shales are common. No evaporites, in particular gypsum, have been reported either in outcrop in the Marsyandi basin (Bordet et al., 1971), or observed in river sediments which provide an integrated signature of rock types in the basin.

Silicate rocks underlie the high relief of the main range, known as the High Himalayan Crystalline Series (HHCS). Two contrasting rock types are present Formation I is dominated by biotite muscovite paragneiss (Le Fort, 1975) and Formation II is dominated by calc-silicates containing diopside, amphibole, quartz and calcite bearing assemblages. Although there is only a relatively small surface area

of HHCS in the Marsyandi basin, small tributaries draining only this unit have been selected as being representative of rivers draining silicate rock.

Dolostones are widespread in the upper Lesser Himalayan Series (LHS) which contains a range of medium to low grade siliclastic and carbonate rocks. A number of small rivers were sampled from this unit and rivers draining specifically dolostone were identified for analysis of Ca and Mg isotope ratios. Carbonates in the LHS are characterised by elevated Sr isotope ratios ($^{87}Sr/^{86}Sr$ ratios in excess of 1) and some of the tributaries analysed in the present study have correspondingly elevated $^{87}Sr/^{86}Sr$ ratios.

2.2. Environmental and ecological gradients

Vegetation can have an important impact on chemical fluxes in rivers because of biomass uptake, and because vegetation impacts upon chemical weathering rates (Drever, 1994; Moulton and Berner, 1998; Moulton et al., 2000; Derry et al., 2005). There is a very strong vegetation gradient across the Marsyandi catchment, linked to precipitation and altitude. The impact of vegetation (in the Marsyandi basin) is undoubtedly complex and is only considered qualitatively here. The degree of vegetation cover has been assessed using the Normalised Difference Vegetation Index (NDVI) (Fig. 1c) (Tucker, 1979) by combining bands 3 and 4 from Landsat images. In the foothills of the main range, rainfall is moderate over the LHS, with 1.6 m of monsoonal rainfall (Burbank et al., 2003). At these altitudes (<500 m) there is dense vegetation (NDVI between 0.5 and 0.85) and all suitable land is terraced, mainly with rice paddies.

Over the HHCS, rainfall is at its highest with >4 m of monsoonal rainfall (Burbank et al., 2003). Vegetation is prominent in the valley bottoms (Fig. 1c) and the valley sides are steep, with frequent slope failure by landslides (e.g. Pratt-Sitaula et al., 2004). The TSS outcrops north of the Annapurna range, mainly at altitudes >3500 m and in the rain shadow of the main range where monsoonal rainfall is <0.5 m (Burbank et al., 2003). The sparse vegetation (NDVI < 0.5) consists of the sedges and grasslands of the Tibetan steppe with only minor terracing and agriculture in the valley bottoms (Fig. 1c).

3. ANALYTICAL METHODS

Samples from the Marsyandi were collected in September 2002 (monsoon) and April 2002 (pre-monsoon) and analysed for *T*, pH, cations and anions and Sr isotope ratios following standard procedures described in Tipper et al. (2006c).

The precise and accurate measurement of Ca and Mg isotopes by MC-ICP-MS have also been described elsewhere (Halicz et al., 1999; Galy et al., 2001; Wieser et al., 2004; Sime et al., 2005; Tipper et al., 2006a) and only a summary is provided here. Mono-elemental solutions of Ca and Mg were obtained by ion-chromatography using Bio-rad AG50W X12 cation exchange resin and Eichrom Sr spec SPS 50–100 μ mesh resin. Column yields were tested by ICP AES, to ensure complete Mg and Ca recovery, and by purifying a multi-elemental solution of known Mg and Ca isotope ratios, to ensure the chemistry did not fractionate isotope ratios. Typically 20 μg of Mg and 100 μg of Ca was processed through chemistry.

The total procedural blanks were <3 ng of Ca and <1 ng of Mg, less than 0.001 of the sample processed. Following chemistry all samples were dissolved in 0.3 N HNO_3 and stored at concentrations in excess of 20 ppm, before centrifugation and introduction in the mass spectrometer. Prior to analysis of Ca and Mg isotope ratios, and following chemistry, levels of Al, Fe, Mn, K, Na, Si and Ca and Mg were monitored to verify chemical purity and quantitative recovery of Ca and Mg.

The Mg and Ca solutions were diluted to the same concentration as the standard (±10%), and introduced into the *Nu* Instruments MC-ICP-MS via an ARIDUS desolvating nebuliser. Both Mg and Ca isotope ratios were analysed using a sample-standard bracketing method (Galy et al., 2001). The $^{26}Mg/^{24}Mg$ is reported in delta notation using the standard formula

$$\delta^{26}\mathrm{Mg} = 1000\left\{\frac{\frac{^{26}\mathrm{Mg}}{^{24}\mathrm{Mg}_{\mathrm{sample}}}}{\frac{^{26}\mathrm{Mg}}{^{24}\mathrm{Mg}_{\mathrm{DSM3}}}} - 1\right\} \quad (1)$$

against the DSM3 standard (Galy et al., 2003). The $^{25}Mg/^{24}Mg$ ratio is also simultaneously analysed to ensure mass dependent behaviour. For comparison, seawater has a $\delta^{26}Mg$ value of −0.82‰ on the DSM3 scale (Chang et al., 2003; Carder et al., 2004; Young and Galy, 2004).

In this study, Ca isotope ratios are normalised to ^{42}Ca following Eisenhauer et al. (2004). Both the $^{44}Ca/^{42}Ca$ and $^{43}Ca/^{42}Ca$ ratios are measured and are reported relative to the NIST SRM915a standard using the conventional notation:

$$\delta^{\frac{44}{42}}\mathrm{Ca} = 1000\left\{\frac{\frac{^{44}\mathrm{Ca}}{^{42}\mathrm{Ca}_{\mathrm{sample}}}}{\frac{^{44}\mathrm{Ca}}{^{42}\mathrm{Ca}_{\mathrm{SRM915a}}}} - 1\right\} \quad (2)$$

Much of the previous work on Ca isotope ratios has reported the $^{44}Ca/^{40}Ca$ ratio relative to various standards. When data from other studies is quoted, it has been converted to $\delta^{44/42}Ca_{SRM915a}$ using the conversions provided in (Sime et al., 2005). Seawater has a $\delta^{\frac{44}{42}}Ca$ of $+0.94 \pm 0.07$‰ relative to the SRM915a standard (Hippler et al., 2003). The range in $^{44}Ca/^{40}Ca$ ratios equals $2.0995 \times {}^{44}Ca/^{42}Ca$ ratios.

The long term reproducibility of Mg isotope ratios was evaluated by repeat analysis of mono-elemental standards, and total procedural replicates through chemistry. Total procedural replicates of synthetic standards of known isotopic composition provide the most robust assessment of accuracy and precision, rather than total procedural replicates of natural samples which only assess the reproducibility. Sixteen total procedural replicates of a multi-elemental standard containing "Cambridge1" Mg were prepared during the period of analysis, and underwent at least duplicate analysis by mass spectrometry. These give a $\delta^{26}Mg$ value (−2.66‰) well inside the 2 SD (2 standard deviation) uncer-

tainty of "Cambridge1" Mg standard (δ^{26} Mg value of −2.60‰) (Tipper et al., 2006a). A conservative estimate of 2SD uncertainty is 0.14‰, from these total procedural replicates.

The reproducibility and accuracy of Ca isotope ratios was monitored by repeat analysis of SRM915a, Specpure and Aristar mono-elemental Ca solutions and total procedural replicates of multi-elemental solutions. The long term reproducibility of $\delta^{\frac{44}{42}}$ Ca values of all standards during the period of analysis for this study was 0.09‰ (2SD), and analysis of multi-elemental standards, made using Aristar Ca yield values within 0.01‰ of analysis of mono-elemental Aristar Ca.

4. RESULTS

Ca and Mg isotope analyses are presented in Table 1. Where referenced, some of this data has already been presented in separate papers but is included here for completeness and clarity. The measured Ca and Mg isotopic composition of the river waters analysed, indicates mass dependent behaviour, defining a mass fractionation line on a 3 isotope plot for both Ca and Mg isotope ratios. For Mg isotopes, deviation from the equilibrium mass fractionation line is expressed as $\Delta^{25}Mg'$ values (Young and Galy, 2004) and for Ca isotope ratios as $\Delta^{43}Ca'$ values (Table 1), following the same notation.

All samples in the present study have a Δ^{25} Mg′ and $\Delta^{43}Ca'$ values within uncertainty of equilibrium mass fractionation (Table 1). The Mg data[1] define a line of gradient 0.517 ± 0.017 ($R^2 = 0.9997$) compared to the theoretical equilibrium gradient of 0.521 (Young et al., 2002). The Ca data define a line with a gradient of 0.54 ± 0.07 ($R^2 = 0.65$) compared to the theoretical line of 0.51 (Sime et al., 2005). Lower abundances of ^{43}Ca than ^{44}Ca and a relatively higher interference on ^{43}Ca from double charged ^{86}Sr, compared to double charged ^{88}Sr on ^{44}Ca, create a larger uncertainty for $\delta^{\frac{43}{42}}$Ca than for $\delta^{\frac{44}{42}}$Ca. $\delta^{\frac{43}{42}}$Ca is not actually used in this study, only reported to demonstrate the mass dependent behaviour of Ca isotope ratios.

The major element and Sr isotope systematics of Himalayan rivers (Tables A1, A2 A3, Appendix A) show similar systematics to previous Himalayan river water studies (e.g. Blum et al., 1998; Galy and France-Lanord, 1999; Galy et al., 1999; Harris et al., 1999; English et al., 2000; Jacobson and Blum, 2000; Evans et al., 2001; Jacobson et al., 2002; Bickle et al., 2003; France-Lanord et al., 2003; Oliver et al., 2003; Quade et al., 2003; Bickle et al., 2005; Tipper et al., 2006c) and are presented only as a comparison to Ca and Mg isotope ratios. Briefly, tributaries from each lithotectonic unit from the Marsyandi basin, have the following characteristics.

TSS tributaries are consistent with limestone weathering, with Ca^{2+} and HCO_3^- as the dominant dissolved ions, but have high Mg/Ca and Sr/Ca molar ratios at 0.78 and 2.84×10^{-3} (Galy and France-Lanord, 1999; Bickle et al., 2005). It has been shown that the high sulphate concentration results from pyrite oxidation, including in the Marsyandi catchment (Galy and France-Lanord, 1999). They exhibit relatively low $^{87}Sr/^{86}Sr$ ratios (mean = 0.717). The major element and Sr isotope chemistry of TSS tributaries in the Marsyandi catchment has been discussed in more detail elsewhere (Evans et al., 2001; Bickle et al., 2005; Tipper et al., 2006c) and is interpreted in the first order to result from a mixture of variable carbonate to silicate weathering. In addition, it has been shown that there is a groundwater contribution to the dissolved load (Tipper et al., 2006c) with a fractionated input of Ca and Mg isotope ratios (Tipper et al., 2006a). Up to 70% of dissolved Ca may be removed by secondary carbonate deposition (Bickle et al., 2005), speculated to fractionate Ca isotope ratios (Tipper et al., 2006a).

HHCS rivers are dilute with an average total dissolved solids (TDS) of 58 mg/l. Rivers draining Formation II (mainly calc-silicate) have low Ca normalised ratios (Mg/Ca < 0.1 and Sr/Ca ~ 1). In Formation I (mainly paragneiss) Ca normalised ratios are higher (Mg/Ca ~ 0.5 and Sr/Ca > 1). $^{87}Sr/^{86}Sr$ ratios are higher than in the TSS, averaging 0.737 reflecting more silicate derived Sr or dissolution of radiogenic carbonate. Hot springs contribute a significant solute flux to HHCS rivers (Evans et al., 2001) and can usually be identified by elevated Cl^- concentrations. The rivers analysed for Ca and Mg isotope ratios in the present study, have been specifically selected to have low Cl^- concentrations and no hot spring correction has been applied to the data. The mean Cl^- of the HHCS tributaries is 15 μmol/l, only a factor of 2 greater than rainfall concentrations and similar to TSS rivers which have a negligible hot spring input.

LHS rivers are concentrated with a TDS of 255 mg/l. The rivers in the present study have been selected to have high Mg/Ca molar ratios (0.6–0.99), reflecting dolomite dissolution. $^{87}Sr/^{86}Sr$ ratios are extremely elevated in these rivers between 0.77 and 0.85, reflecting the Proterozoic age of the source rock and metamorphic exchange of Sr into more readily dissolvable carbonate phases (Bickle et al., 2001).

4.1. Ca and Mg isotope ratios in Himalayan rocks and small mono-lithological rivers

Mg isotope data are available on each of the three main rock reservoirs (limestone, silicate and dolostone) from the Marsyandi catchment (Galy et al., 2002; Tipper et al., 2006a). The three rock reservoirs have distinct δ^{26}Mg values (Fig. 2a–c). Small rivers draining each rock type differ in their δ^{26}Mg values from the δ^{26}Mg values of the rocks (Fig. 2a–c) but the offsets vary with rock type. Small rivers draining limestone have, on average, a δ^{26}Mg value which is 1.4‰ greater than the average limestone value (Fig. 2c), whereas rivers draining mainly silicate rock have a δ^{26} Mg value on average 0.9‰ lower than the average rock value (Fig. 2b). The hot springs of the mainly silicate HHCS have a δ^{26}Mg value close to that of silicate rock. However, small rivers draining dolostone have a δ^{26}Mg value within analytical uncertainty of dolostone δ^{26}Mg values (Fig. 2a).

Similar, though less marked discrepancies between rock and river are observed for Ca isotope ratios. Ca isotope

[1] The gradient is calculated by regressing $\delta^{26}Mg'$ and δ^{25} Mg′ following Young and Galy (2004).

Table 1
Ca and Mg isotope data on Himalayan river waters

	Catchment	$\delta^{26}Mg \pm 2\sigma_m$	$\delta^{25}Mg \pm 2\sigma_m$	$\Delta^{25}Mg'$	N	$\delta^{44}_{42}Ca \pm 2\sigma_m$	$\delta^{43}_{42}Ca \pm 2\sigma_m$	$\Delta^{43}Ca'$	N
LHS tributaries									
ett2	Marsyandi	−1.30 ± 0.00	−0.67 ± 0.03	0.00	2	0.61 ± 0.07	0.21 ± 0.14	−0.10	2
ett149	Marsyandi	−1.14 ± 0.06	−0.57 ± 0.01	0.02	2	0.67 ± 0.03	0.28 ± 0.03	−0.06	2
ett150	Marsyandi	−1.29 ± 0.01	−0.65 ± 0.04	0.02	2	0.53 ± 0.06	0.24 ± 0.02	−0.03	2
ett151	Marsyandi	−1.31 ± 0.09	−0.70 ± 0.05	−0.02	3	0.47 ± 0.13	0.36 ± 0.17	0.12	3
ett153[b]	Marsyandi	−1.39 ± 0.08	−0.73 ± 0.04	0.00	3	0.81 ± 0.07	0.41 ± 0.04	0.00	2
ct59	Marsyandi	−1.39 ± 0.03	−0.72 ± 0.03	0.01	3	0.58 ± 0.08	0.42 ± 0.20	0.12	2
NH7[b]	Andhi	−1.35 ± 0.08	−0.69 ± 0.06	0.01	3	0.82 ± 0.04	0.44 ± 0.06	0.02	3
LHS mean		−1.31 ± 0.07	−0.68 ± 0.04	0.01	7	0.64 ± 0.10	0.34 ± 0.07	0.01	7
HHCS tributaries and silicate dominated rivers									
ett70	Marsyandi	−1.56 ± 0.06	−0.81 ± 0.03	0.01	2	0.44 ± 0.06	0.28 ± 0.20	0.05	2
ett96	Marsyandi	−1.29 ± 0.02	−0.69 ± 0.02	−0.02	2	0.36 ± 0.07	0.16 ± 0.19	−0.02	3
ett96rep	Marsyandi	−1.20 ± 0.10	−0.62 ± 0.07	0.00	1	0.44 ± 0.09	0.16 ± 0.23	−0.07	2
ett136	Marsyandi	−1.43 ± 0.03	−0.75 ± 0.02	0.00	2	0.40 ± 0.05	0.20 ± 0.12	−0.01	2
Mo308	Marsyandi	−1.15 ± 0.11	−0.62 ± 0.06	−0.03	3	0.33 ± 0.14	0.07 ± 0.11	−0.11	2
Mo316[b]	Marsyandi	−0.78 ± 0.08	−0.40 ± 0.03	0.01	3	0.36 ± 0.02	0.01 ± 0.17	−0.17	3
TO320	Trisuli	−1.36 ± 0.14	−0.70 ± 0.06	0.01	3	0.39 ± 0.31	0.21 ± 0.40	0.01	2
HHCS mean		−1.25 ± 0.22	−0.66 ± 0.12	0.00	6	0.39 ± 0.03	0.15 ± 0.08	−0.05	6
ace33[b]	Tibet	−0.75 ± 0.09	−0.41 ± 0.07	0.01	4	0.33 ± 0.07	0.21 ± 0.12	0.04	2
TSS tributaries									
ace68	Arun	−1.43 ± 0.12	−0.76 ± 0.11	−0.02	3	0.35 ± 0.06	0.13 ± 0.10	−0.05	2
ett17	Marsyandi	−0.77 ± 0.01	−0.38 ± 0.01	0.02	3	0.29 ± 0.07	0.12 ± 0.10	−0.02	3
ett23	Marsyandi	−1.32 ± 0.05	−0.68 ± 0.03	0.01	2	0.36 ± 0.05	0.22 ± 0.02	0.03	2
ett24	Marsyandi	−0.81 ± 0.09	−0.43 ± 0.02	0.00	3	0.45 ± 0.03	0.33 ± 0.11	0.10	2
ett27	Marsyandi	−1.45 ± 0.00	−0.74 ± 0.01	0.01	3	0.62 ± 0.06	0.22 ± 0.11	−0.12	3
ett30	Marsyandi	−1.22 ± 0.07	−0.61 ± 0.10	0.02	3	0.29 ± 0.07	0.12 ± 0.05	−0.03	2
ett38	Marsyandi	−1.60 ± 0.05	−0.84 ± 0.03	−0.01	2	0.21 ± 0.01	0.15 ± 0.07	0.04	2
ett58	Marsyandi	−1.41 ± 0.03	−0.76 ± 0.01	−0.02	3	0.41 ± 0.02	0.24 ± 0.22	0.03	2
ett59	Marsyandi	−1.50 ± 0.09	−0.77 ± 0.07	0.01	3	0.47 ± 0.04	0.37 ± 0.10	0.13	2
ett61	Marsyandi	−1.72 ± 0.09	−0.91 ± 0.03	−0.01	3	0.49 ± 0.07	0.26 ± 0.06	0.01	2
MT113	Nar	−1.16 ± 0.03	−0.61 ± 0.05	0.00	4	0.38 ± 0.04	0.11 ± 0.16	−0.09	2
MT2	Nar	−1.21 ± 0.08	−0.65 ± 0.07	−0.02	4	0.24 ± 0.06	0.18 ± 0.08	0.06	3
ett74	Nar	−1.19 ± 0.05	−0.61 ± 0.00	0.00	2	0.38 ± 0.03	0.17 ± 0.09	−0.03	3
ett74rep	Nar	−1.19 ± 0.06	−0.63 ± 0.09	−0.01	2	0.41 ± 0.03	0.25 ± 0.14	0.04	2
TSS mean		−1.36 ± 0.17	−0.71 ± 0.09	0.00	1	0.38 ± 0.05	0.21 ± 0.04	0.01	13
Marsyandi main river									
ett1	Marsyandi	−1.38 ± 0.10	−0.70 ± 0.05	0.01	4	0.28 ± 0.04	0.02 ± 0.05	−0.12	2
ett22	Marsyandi	−1.69 ± 0.09	−0.86 ± 0.09	0.03	3	0.37 ± 0.02	0.14 ± 0.13	−0.05	2
ett43	Marsyandi	−2.08 ± 0.08	−1.08 ± 0.02	0.01	3	0.41 ± 0.04	0.28 ± 0.05	0.07	3
ett69[a]	Marsyandi	−1.75 ± 0.03	−0.90 ± 0.04	0.01	2	0.42 ± 0.04	0.23 ± 0.03	0.02	3
ett69rep[a]	Marsyandi	−1.61 ± 0.09	−0.84 ± 0.09	0.01	3	0.41 ± 0.04	0.25 ± 0.20	0.04	2
ett84	Marsyandi	−1.80 ± 0.08	−0.90 ± 0.03	0.04	3	na	na	na	na
ett155	Marsyandi	−1.34 ± 0.06	−0.71 ± 0.02	−0.01	3	0.35 ± 0.05	0.08 ± 0.02	−0.10	2
Large rivers									
BGP4[b]	Ganges	−1.20 ± 0.06	−0.64 ± 0.01	−0.02	3	0.31 ± 0.01	0.04 ± 0.00	−0.12	2
BR213[b]	Ganges	−1.39 ± 0.06	−0.70 ± 0.09	0.02	3	0.28 ± 0.05	0.08 ± 0.16	−0.06	3
ett164[b]	Trisuli	−1.29 ± 0.03	−0.68 ± 0.02	−0.01	2	0.55 ± 0.05	0.23 ± 0.14	−0.05	2
ett164[b] rep	Trisuli	−1.43 ± 0.11	−0.76 ± 0.04	−0.01	2	0.53 ± 0.09	−0.04 ± 0.51	−0.31	1
NAG14[b]	Bheri	−1.19 ± 0.16	−0.62 ± 0.13	0.00	2	0.40 ± 0.08	0.11 ± 0.23	−0.10	3
NAG45[b]	Kali Gandaki	−1.54 ± 0.03	−0.80 ± 0.03	0.00	3	0.36 ± 0.01	0.10 ± 0.08	−0.09	2
NAG49[b]	Narayani	−1.33 ± 0.04	−0.68 ± 0.02	0.01	3	0.47 ± 0.00	0.14 ± 0.07	−0.10	2
ace158[b]	Mekong	−1.03 ± 0.08	−0.54 ± 0.04	0.03	6	0.50 ± 0.07	0.20 ± 0.23	−0.06	2
Hot springs									
HS7	Marsyandi	−0.87 ± 0.04	−0.46 ± 0.01	0.00	3	na	na	na	na
HS9	Marsyandi	−0.05 ± 0.02	−0.03 ± 0.02	−0.01	2	0.52 ± 0.00	0.16 ± 0.01	−0.11	2

Table 1 (*continued*)

Catchment	$\delta^{26}Mg \pm 2\sigma_m$	$\delta^{25}Mg \pm 2\sigma_m$	$\Delta^{25}Mg'$	N	$\delta^{44}_{42}Ca \pm 2\sigma_m$	$\delta^{43}_{42}Ca \pm 2\sigma_m$	$\Delta^{43}Ca'$	N
Dolostone rock								
AP207[c]	−1.38 ± 0.05	−0.71 ± 0.06	0.01	3	0.74 ± 0.11	0.46 ± 0.17	0.08	1
AP867[c]	−1.34 ± 0.11	−0.68 ± 0.05	0.02	3	0.67 ± 0.03	0.30 ± 0.15	−0.04	1
AP865[c]	−1.66 ± 0.07	−0.85 ± 0.03	0.02	3	0.71 ± 0.06	0.32 ± 0.13	−0.04	1

N is the number of analyses by mass spectrometry and na is not analysed. $2\sigma_m$ is the external error (2SD) divided by the square root of the number of replicates (N).

[a] $\delta^{26}Mg$ values originally reported in Tipper et al. (2006a).

[b] $\delta^{26}Mg$ values already published in Tipper et al. (2006b).

[c] $\delta^{26}Mg$ values originally reported in Galy et al. (2002) and converted to the DSM3 scale in Young and Galy (2004).

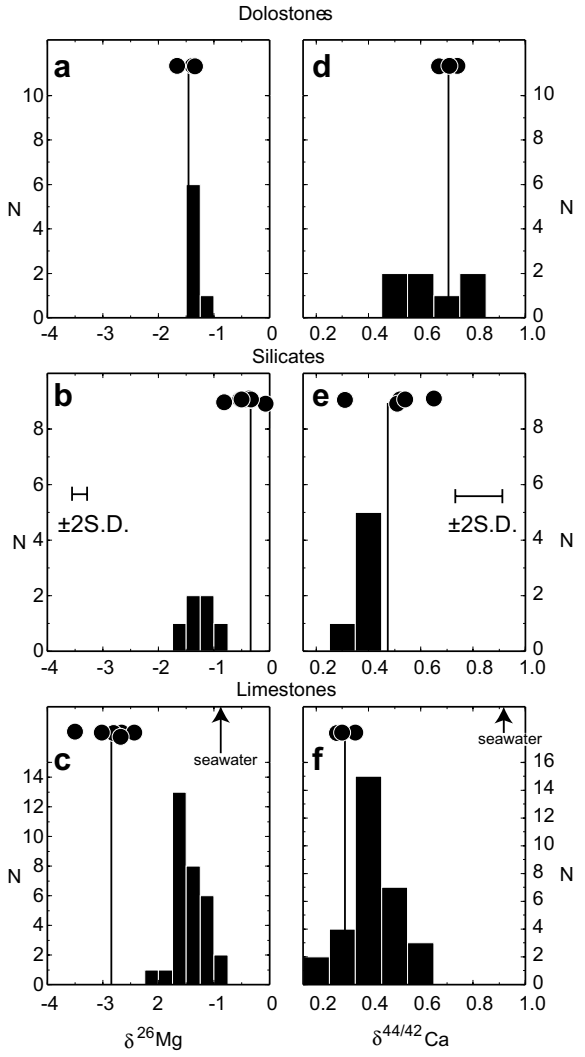

Fig. 2. Summary of Mg and Ca isotope data in small tributaries (histograms) and rock samples (circles) from the Marsyandi basin. The mean of the rock data is indicated by the vertical line for each rock type. Rock data is from Galy et al. (2002), Tipper et al. (2006a) and the present study. Himalayan river water data from Tipper et al. (2006a) is included in the histograms. Seawater compositions are also shown for comparison.

data is already available for limestone and silicate rock in the Marsyandi basin (Tipper et al., 2006a), but the $\delta^{44}_{42}Ca$ measurements of dolostone presented here are new. Dolostone from the Marsyandi has an average $\delta^{44}_{42}Ca$ value of 0.71‰, distinct from both limestone and silicate rock. These are some of the most elevated $\delta^{44}_{42}Ca$ values in rocks reported so far. These LHS dolomites also have extremely elevated $^{87}Sr/^{86}Sr$ ratios at ca. 0.8 (Singh et al., 1998; Galy et al., 1999; Bickle et al., 2001). The elevated $^{87}Sr/^{86}Sr$ ratios in these rocks results from metamorphic exchange with silicate ^{87}Sr, Sr which has its $^{87}Sr/^{86}Sr$ ratio elevated by decay of ^{87}Rb (Bickle et al., 2001). Zhu and Macdougall (1998) noted that tributaries of the Ganges had low $^{44}Ca/^{40}Ca$ ratios, which may result from decay of ^{40}K to ^{40}Ca in LHS rocks (DePaolo, 2004), leading to low ratios in a similar way to ^{87}Rb decaying to ^{87}Sr leads to high $^{87}Sr/^{86}Sr$. This cannot be the case for $\delta^{44}_{42}Ca$ values as neither ^{44}Ca and ^{42}Ca are the products of radioactive decay, implying that either the $\delta^{44}_{42}Ca$ values are original or have exchanged with a source of Ca having elevated $\delta^{44}_{42}Ca$ values. Since the 3 dolostone samples have identical $\delta^{44}_{42}Ca$ values at the 95% confidence level whereas they have witnessed variable degree of metamorphic exchange as their $^{87}Sr/^{86}Sr$ ratios range from 0.7395 to 0.8572 (Galy et al., 1999), it is likely that this elevated Ca isotopic signature is inherited from the sedimentary origin of these rocks. Small rivers draining these dolostones have similar $\delta^{44}_{42}Ca$ values to the dolostone (Fig. 2d). However, small rivers draining limestone show a tendency towards elevated $\delta^{44}_{42}Ca$ values compared to rock (Fig. 2f). Small rivers draining silicate rock are within the range of silicate rock $\delta^{44}_{42}Ca$ values, but have a lower average $\delta^{44}_{42}Ca$ value than the rock (Fig. 2e).

The difficulty in interpreting such differences between isotope ratios in rock and waters is that they may arise either as a result of mixtures between inherited lithological signatures (i.e. from a mixture between limestone, silicate or dolomite derived Ca and Mg), or as a result of fractionation during weathering processes. A multi-tracer approach, linking major dissolved ions and Ca and Mg isotope ratios in the Marsyandi catchment allows this difficulty between inherited isotope signatures and process related signatures to be considered in more detail. Much of what follows in the discussion relates to the controls of Ca and Mg isotope ratios in river waters.

4.2. Ca and Mg isotope ratios in the Marsyandi mainstem

The downstream profiles of both Ca and Mg isotopes ratios in the mainstem of Marsyandi River and tributaries (Fig. 3a and b) evolve over the 150 km from the headwaters

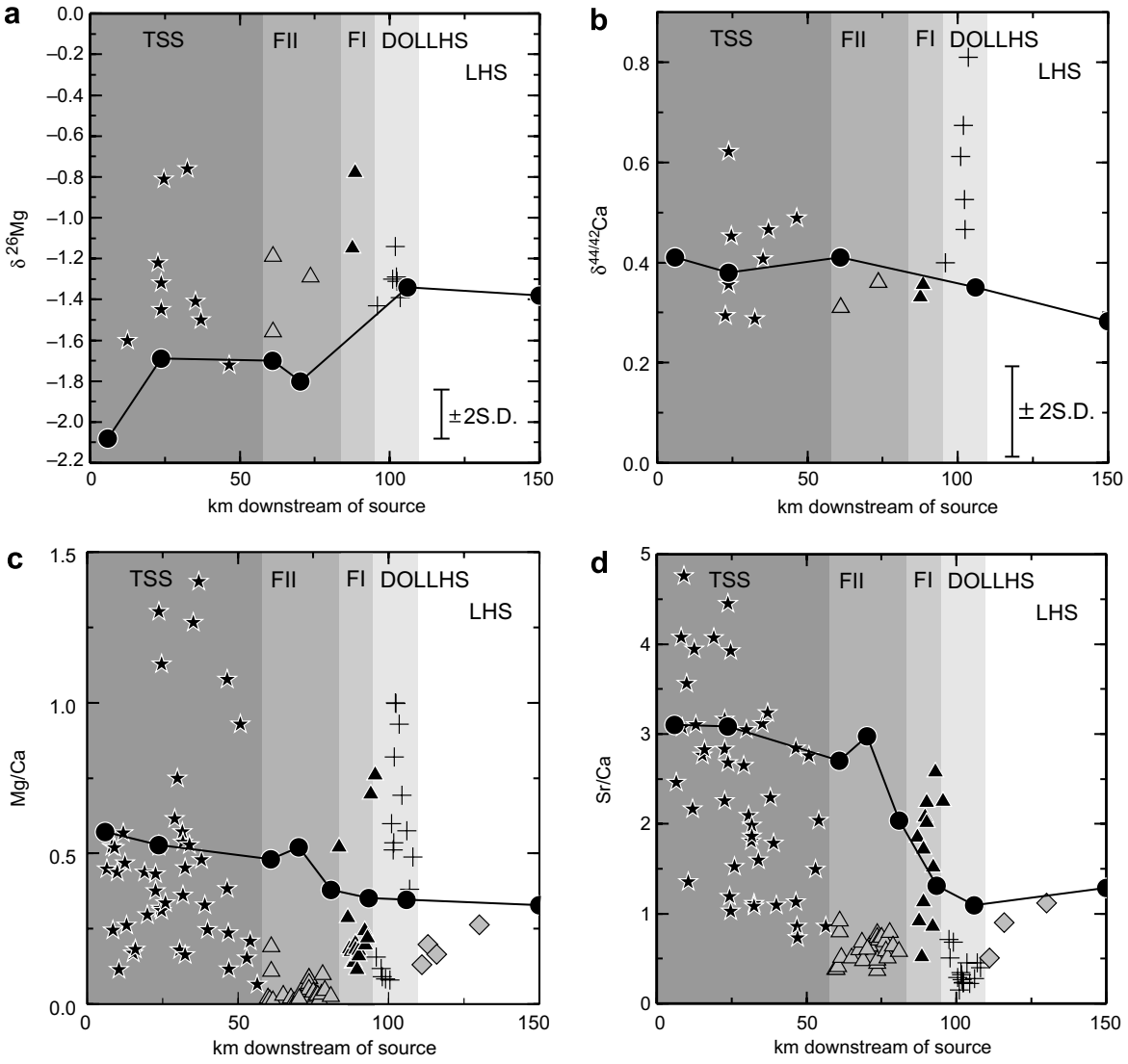

Fig. 3. Downstream profiles in the Marsyandi. (a) Mg isotope ratios, (b) Ca isotope ratios, (c) Mg/Ca ratios, (d) Sr/Ca ratios. The solid black line links the mainstem samples for the downstream profile. The shading defines the main lithological types, with the HHCS divided into its two main formations. The LHS has been divided into two units, dolomitic (DOLLHS) and non-dolomitic (LHS).

to the confluence with the Trisuli. δ^{26}Mg values increase monotonically by 0.7‰ from the headwaters to the furthest sample downstream analysed and the mainstem has lower δ^{26}Mg values than nearly all the tributaries (Fig. 3a). Once the Marsyandi has left the TSS, this reflects the fact that the river is buffered by the concentrated input from the TSS, with an addition of a more dilute input from the HHCS and LHS having a limited effect. However, in the TSS the main river is by definition a mixture of these headwater tributaries, and it is surprising that the main river has a lower δ^{26}Mg value than all but one of the tributaries analysed. This may have arisen as an artifact from the small sample set ($n = 9$). However, a much larger data set is available for Mg/Ca ratios and indicates that sample bias cannot account for the difference between the mainstem and the tributaries, because the mainstem has a higher Mg/Ca than all but 10 tributaries (Fig. 3d). These tributaries with Mg/Ca close to unity are known to drain black shale with elevated Mg/Ca ratios. These are however very small tributaries, and it would be surprising if they had a significant impact on the chemistry of the main river.

These Mg/Ca and Mg isotope ratios imply that there must be an alternative source of Mg or Ca to the Marsyandi River, other than the tributaries, or that Mg is not conservative in the Marsyandi river. In other publications, Tipper et al. (2006a,c) have argued that there must be a groundwater input to the Marsyandi in the TSS, which could account for the discrepancy in δ^{26}Mg values between the main river and the tributary δ^{26}Mg values. It should be noted that a similar discrepancy between mainstem and tributaries have been reported from the adjacent Kali Gandaki catchment, where the mainstem has a (^{234}U/^{238}U) ratio

>0.98 whereas the tributaries are always lower than 0.971 (Chabaux et al., 2001).

Ca isotope ratios appear to decrease slightly along the downstream profile but all samples are within 2SD uncertainty. The elevated $\delta^{\frac{44}{42}}$Ca values of the LHS tributaries has no impact on the $\delta^{\frac{44}{42}}$Ca value of the main river, which is consistent with the small surface area of the dolostone in the upper LHS. The Sr/Ca and Mg/Ca ratios of the downstream profile are presented for comparison with the Ca and Mg isotope data. There are large differences between lithological types for these elemental ratios in the tributaries (Fig. 3c and d), because of the large range in elemental ratios in each rock type (compared to isotope ratios).

4.3. Ca and Mg isotope ratios in large Himalayan rivers

The δ^{26}Mg values of the large rivers considered here has already been reported (Tipper et al., 2006b) but the Ca isotope data is new, and the Himalayan tributary data permit the δ^{26}Mg and $\delta^{\frac{44}{42}}$Ca data to be considered in a regional context. The average δ^{26}Mg value of the large Nepalese tributaries is $-1.39‰$, within analytical uncertainty of the tributary data from each of the main lithotectonic units, but closest to δ^{26}Mg values in tributaries draining limestone from the TSS. The large tributaries of the Ganges have a δ^{26}Mg value within uncertainty of the Ganges itself, suggesting that Mg isotope ratios are largely conserved from headwaters to mouth. The headwaters of the Mekong in Tibet has a higher δ^{26}Mg value than the Ganges at $-1.03‰$.

For Ca isotopes, the two samples of the Ganges from the monsoon season are in very close agreement averaging $0.30 \pm 0.03‰$. However, these samples are significantly different from the dry season sample of Schmitt et al. (2003) at $0.55‰$. $\delta^{\frac{44}{42}}$Ca values in the Ganges are slightly lower than the average of its large tributaries (Narayani, Kali Gandaki, Bheri and Trisuli) which average $0.46 \pm 0.07‰$, but these tributaries were collected in the dry season, and are closer to the $\delta^{\frac{44}{42}}$Ca value from Schmitt et al. (2003). The average of the these large tributaries in the Narayani system is within the range of $\delta^{\frac{44}{42}}$Ca values for the Marsyandi tributaries.

5. DISCUSSION: CONTROLS ON SOLUTE CA AND MG ISOTOPE RATIOS IN TRIBUTARIES

The isotopic composition of natural waters is controlled by mixtures of waters with distinct isotopic compositions, reflecting the diversity of bedrock (e.g. Gaillardet et al., 1999) as well as fractionation during weathering. Recent work has confirmed that the isotope ratios of Ca and Mg can be fractionated in the weathering environment (Galy et al., 2002; Schmitt et al., 2003; Wiegand et al., 2005; Tipper et al., 2006a,b). In the headwaters of the Marsyandi river, Ca and Mg isotope ratios were interpreted to be controlled by fractionation from bedrock isotope ratios (Tipper et al., 2006a) based on small seasonal variations, and a discrepancy between bedrock and solute isotopic compositions. However, a global compilation of Mg isotope ratios in small rivers has revealed clear differences in δ^{26}Mg values of solute Mg between rivers draining limestone and silicate rock, whilst in large rivers from across the world there was no obvious lithological control of δ^{26}Mg values (Tipper et al., 2006b). The contrasting isotope signatures of the Marsyandi bedrock permit a more detailed evaluation of the lithological control of Ca and Mg isotope ratios in rivers.

5.1. Lithological control of solute Ca and Mg isotope ratios

The lithological control of riverine chemistry can be represented on element-ratio diagrams where tributary data plots on mixing arrays. In the Marsyandi catchment, tributary chemistry can be modelled as a binary mixture between a "carbonate-like" end-member and a "silicate-like" end-member (Bickle et al., 2005). Such mixing arrays are illustrated for the tributaries in the Marsyandi catchment (Fig. 4a–c) using Sr/Na and Na/Ca ratios. For each lithotectonic unit, the tributaries define hyperbolic arrays, interpreted as mixtures between different end-members (Bickle et al., 2005). In the case that Ca and Mg isotopes are controlled by mixtures between lithological end-members, it is anticipated that Ca and Mg isotope ratios should plot on similar two component mixing arrays to elemental ratios, and that end-members can be extrapolated from such a plot.

The tributaries analysed for Ca and Mg isotope ratios (the stars on Fig. 4a–c) were specifically selected to be representative of the mixing arrays defined by the major element ratios, with the exception of LHS tributaries which do not span the mixing array defined by all LHS tributaries (Fig. 4a). These LHS tributaries were selected as being representative of dolomite weathering.

When tributary δ^{26}Mg values are compared to Na/Ca ratios, it is evident that the data do not define two component mixing arrays (Fig. 4d–f) and end-members cannot be inferred, contrary to major element ratios. This strongly suggests that Mg isotope ratios cannot be explained by simple mixtures between components derived from carbonate and silicate end-members. The lack of lithological control is further evident for Mg isotope ratios, when one considers that the average of the tributaries draining each main lithology have δ^{26}Mg values within the uncertainty of the method, whilst the lithologies have distinct δ^{26}Mg values.

Hot springs provide a concentrated chemical flux to HHCS tributaries and are not always associated with high Cl^- concentrations (Evans et al., 2004; Becker, 2005). Therefore, they could potentially have an important control on solute Mg and Ca isotope ratios in some tributaries. The δ^{26}Mg values of the hot springs are distinct from the tributary δ^{26}Mg values (Fig. 4e) suggesting that the influence of hot springs is not significant, at least for the selected tributaries which have been analysed.

There is no correlation between Na/Ca ratios and $\delta^{\frac{44}{42}}$Ca values (Fig. 4g–i), suggesting that variability in rock $\delta^{\frac{44}{42}}$Ca values is not the major cause of variability in the $\delta^{\frac{44}{42}}$Ca values of solute Ca. Moreover, in the TSS, solute Ca in rivers is buffered by limestone dissolution, but there is a wide range of $\delta^{\frac{44}{42}}$Ca values in the tributaries compared to lime-

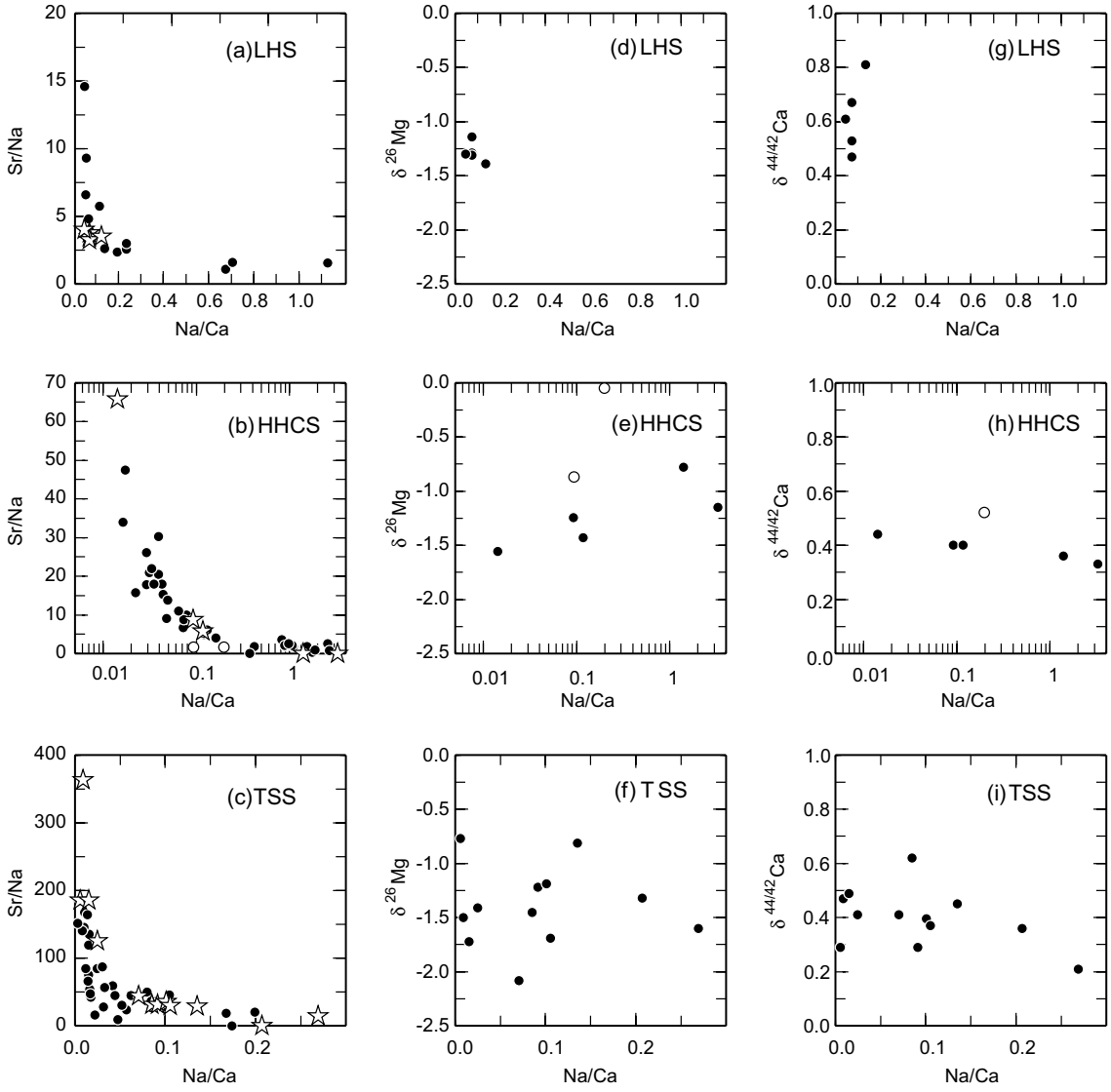

Fig. 4. The relationship between major element ratios and Mg and Ca isotope ratios in Marsyandi tributaries. The black circles are tributaries, and the stars are tributaries that were selected for Ca and Mg isotope analysis. Unfilled circles are hot springs. The upper plots are for the LHS (dolostone), middle plots are for the HHCS (silicate) and lower plots are for the TSS (limestone). Note the log scale for the HHCS plots, but that an array is still observed.

stone $\delta^{\frac{44}{42}}$Ca values, with the average of the rock distinct from the average of the water. It is, however, worth remembering that small rivers draining dolostone in the LHS have δ^{26}Mg and $\delta^{\frac{44}{42}}$Ca values, identical to the dolostone isotopic composition (Fig. 2a and d) within the uncertainty of the method. Therefore, the lithology certainly influences the isotopic composition of solute Ca and Mg, but at the scale of the whole Himalayan range, isotopic fractionation during weathering appears to have a significant impact on isotopic compositions of the solute elements.

5.2. Fractionation control of solute Ca and Mg isotope ratios

There are several plausible mechanisms which could fractionate Ca and Mg during weathering, including, incorporation of Ca and Mg into biomass (Schmitt et al., 2003; Wiegand et al., 2005; Black et al., 2006), precipitation of secondary carbonate and precipitation of clay phases during incongruent weathering (Tipper et al., 2006a). Here, we re-evaluate the probable fractionation control of solute Ca and Mg isotope ratios.

The most convincing evidence for Mg isotope fractionation comes from the small tributaries draining the HHCS (silicate) with δ^{26}Mg values, which are on average 0.63‰ lower than that of the silicate rock (Fig. 5). Soil developed from Formation I (paragneiss) has been reported with δ^{26}Mg values up to 0.5‰ higher than in Formation I bedrock (Tipper et al., 2006a), consistent with Mg isotope ratios being fractionated during silicate weathering (Tipper et al., 2006a). We speculate that this shift towards elevated

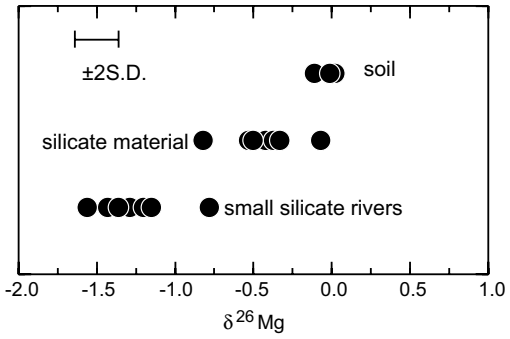

Fig. 5. δ^{26}Mg values of silicate material, small tributaries draining silicate rock from the Marsyandi HHCS and soil. Silicate material and soil data is from the Marsyandi HHCS (Tipper et al., 2006a).

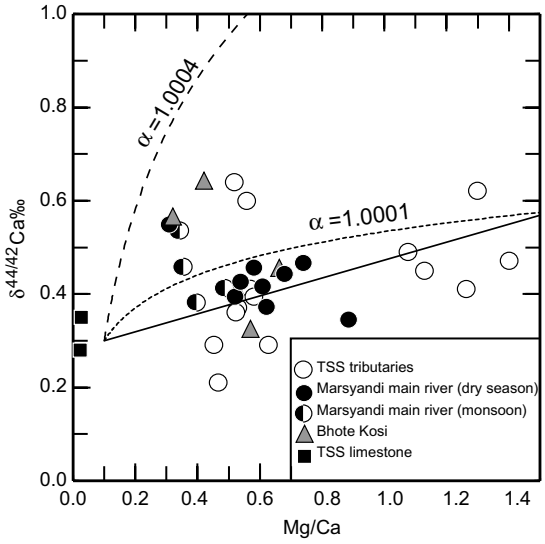

Fig. 6. Rayleigh fractionation for $\alpha^{Ca}_{water-calcite}$ 1.0001 and 1.0004 (dotted and dashed curves, respectively). The starting point corresponds to the Ca isotopic composition of the limestone whereas the Mg/Ca ratio has been increased to account for silicate derived Mg in the water. The solid curve schematically represents a mixing line, between fractionated waters and waters which have a lithological chemical signature. Data is from Tipper et al. (2006a) and the present study.

δ^{26}Mg values occurs during the formation of secondary clay phases. If soil preferentially retains Mg with high δ^{26}Mg values during silicate weathering, then the solute complement should have low δ^{26}Mg values as a consequence of silicate weathering, as is observed in the small tributaries. Given that the amount of Mg exported from the catchment as solute Mg is <2% of the total amount of Mg transported by Himalayan rivers (solute and particulate) (Galy and France-Lanord, 1999), this $\Delta^{26}Mg_{silicate-dissolved}$ value of ca. −0.63‰ (from −0.21 to −1.15 including uncertainties) corresponds to an isotopic fractionation factor ($\alpha^{Mg}_{silicate-dissolved}$) of 0.99937 between solute and residual Mg during the incongruent weathering of silicate rocks, and is similar to a previous estimate of 0.9985 to 0.9995 (Tipper et al., 2006b). It is worth noticing that the δ^{26}Mg values of the hot springs are closer to rock values than most of the riverine δ^{26}Mg values, suggesting that the Mg isotopic fractionation factor during the incongruent weathering of silicate rocks is likely to follow the Arrenhius ($\sim 1/T$) temperature relationship.

The most probable mechanism which fractionates Ca isotope ratios is the precipitation of secondary calcite (Tipper et al., 2006a). Up to 70% of Ca is estimated to be lost from Himalayan rivers (Galy et al., 1999; Jacobson et al., 2002; Bickle et al., 2005), particularly in TSS rivers in the arid climate of the Tibetan Plateau. Groundwater, associated with travertine deposition, has been demonstrated to be fractionated to higher δ^{44}_{42}Ca values, with the travertine complement having lower δ^{44}_{42}Ca values (Tipper et al., 2006a). We speculate that the range in δ^{44}_{42}Ca values observed in the present data set can be reconciled by mixtures between waters which have undergone variable amounts of calcite precipitation (Fig. 6). There is no quantitative relationship between Ca concentrations and δ^{44}_{42}Ca values as may be anticipated, but it is probable that the fractionation factor between water and calcite is variable because of a kinetic limitation (Lemarchand et al., 2004).

The contrast in vegetation density between the TSS and the LHS allows a preliminary assessment of the impact vegetation has on Ca and Mg isotope ratios in rivers. The storage of Ca with low δ^{44}_{42}Ca values in biomass may be a mechanism for enriching solute Ca with high δ^{44}_{42}Ca values (Schmitt et al., 2003; Wiegand et al., 2005) and Mg isotope ratios have been demonstrated to be fractionated by chlorophyll-a (Black et al., 2006). If vegetation has a strong influence on solute δ^{26}Mg and δ^{44}_{42}Ca values, then a difference between rock and tributary δ^{26}Mg values is anticipated to be observed in catchments with dense vegetation. In the densely vegetated LHS (NDVI between 0.5 and 0.85), the δ^{26}Mg and δ^{44}_{42}Ca values of the dissolved load are within analytical uncertainty of the bedrock. The simplest interpretation of these isotope ratios is that they are inherited from the congruent dissolution of dolostone. In contrast, and somewhat counter intuitively, in the sparsely vegetated TSS (NDVI <0.5), the solute δ^{26}Mg and δ^{44}_{42}Ca values are distinct from the limestone bedrock. However, the vegetation type is poorly documented in the Marsyandi basin and the NDVI (Fig. 1c) is likely to exhibit strong seasonal variations, preventing at present any quantitative interpretation of the role of vegetation for Ca and Mg isotope ratios. Nevertheless, a concomitant effect of the vegetation would enrich Ca and Mg isotope ratios in the dissolved component to higher δ^{44}_{42}Ca and δ^{26}Mg values, because both Ca and Mg in organic matter are enriched in the light isotopes (Wiegand et al., 2005; Black et al., 2006). Therefore, our data from small tributaries suggests that either, the biological cycle of Mg and Ca are decoupled at a catchment scale or that the scale of the isotopic fractionation associated with the alkali-earths in the biosphere is not large enough to dominate the isotopic signal of the riverine dissolved load. With the current riverine data set available, it is not possible to reach a final conclusion about the role of vegetation on Ca and Mg isotope ratios in rivers.

In the main river of the Marsyandi at Chame (just below the TSS), it has recently been noted that Ca and Mg isotope ratios define an array over a seasonal cycle (Tipper et al., 2006a). This was interpreted to reflect a fractionated input of groundwater. Whilst we suspect that this is also the case in many of the tributaries analysed in the present study, it is neither expected nor generally observed to be the case that Ca and Mg isotope ratios define an array, unless a single system is considered. Each separate tributary behaves in a different way depending on the degree of fractionation, the starting composition and the volume of groundwater input to the system.

6. IMPLICATIONS AND GLOBAL PERSPECTIVES

The lack of simple relationship between riverine δ^{26}Mg values and elemental ratios such as Na/Ca, commonly used to trace source lithology in river waters, confirms observations from large rivers across the globe where no correlation between δ^{26}Mg values and $^{87}Sr/^{86}Sr$ or $Si(OH)_4$/Ca ratios has been observed (Tipper et al., 2006b). Indeed, the average of tributaries draining three distinct lithologies presented here, is within the uncertainty of the method. Therefore, any lithological signature is masked. The data from the small silicate HHCS tributaries is consistent with earlier reports of fractionation of Mg isotopes during weathering (Tipper et al., 2006a). Mg isotope ratios in river waters therefore have, at least a dual control: a difference in source lithology, and fractionation during weathering, making riverine δ^{26}Mg values complicated to interpret. It seems unlikely that Mg isotope ratios will prove useful as a tracer of carbonate to silicate dissolution because of the fractionation during silicate weathering, and because of the large range of δ^{26}Mg values present in carbonate rocks (Galy et al., 2002). Nevertheless, δ^{26}Mg values can still be used to place some new constraints on the origin of Mg in TSS rivers. Considering that the average δ^{26}Mg value of the rivers draining limestone is 1.4‰ greater than the average limestone value (Fig. 2c), and that the average difference in the δ^{26}Mg value of limestone and silicate rock is 2.16‰, mass balance implies that at least 50% of the Mg is derived from silicate weathering in those catchments. This estimate is a minimum value because this does not take into account the fractionation of δ^{26}Mg values during incongruent silicate weathering. If we consider the Mg isotope fractionation factor between solute and clay phases estimated in the HHCS catchment, the proportion of Mg derived from silicate weathering in the TSS could be as high as 90%. These estimates must be treated with caution given (1) the significant heterogeneity of the 2 end-members and (2) the use of an isotopic fractionation factor with an even greater uncertainty. They do however illustrate the future potential of Mg isotope data, through detailed studies at a small scale, to refine the current understanding about the origin of Mg.

The characterisation and quantification of the incongruent dissolution of silicates (and carbonates) will be useful for constraining the origin of solute elemental ratios, and help correct them in order to quantify the source of river alkalinity more accurately. Although the range in some elemental ratios is so large between rock types, that contrasts in rivers draining different rock types can still be detectable (Figs. 3(d and c), and 4), the implication from the Ca and Mg isotope ratios in the present work is that Ca and Mg have been recycled by processes, and therefore do not directly reflect rock ratios. This confirms that the deconvolution of the riverine elemental compositions (Bickle et al., 2003, 2005) into end-members does not necessarily quantify the rock contribution directly. For instance, precipitation of 70% of the Ca as secondary calcite, drastically modifying elemental ratios, (e.g. Galy et al., 1999; Jacobson et al., 2002; Bickle et al., 2005) would elevate the solute δ^{44}_{42}Ca values by the observed ~0.13‰, if the water–calcite fractionation factor was ~0.1‰ (the two curves on Fig. 6 model the evolution of water compositions during precipitation of calcite, assuming no re-dissolution). The data from rivers draining limestone can be explained remarkably well by such a simple model in Mg/Ca versus δ^{44}_{42}Ca space (Fig. 6), where precipitation of calcite creates a fractionated end-member, which then mixes with a rock-like end-member (dashed line). The modelling of the data requires a $^{44/42}$Ca isotopic fractionation ($\alpha^{Ca}_{water-calcite}$) factor of 1.0001 and would suggest that calcite precipitated in the Marsyandi are less fractionated than the travertines from the Bhote Kosi, which would require a $^{44/42}$Ca isotopic fractionation factor of 1.0004 in order to have precipitated from the modern water (Tipper et al., 2006a). Given that Ca-isotope fractionation factors are precipitation-rate dependent (Lemarchand et al., 2004), this may reflect faster precipitation in the environment that controls the water chemistry. In particular, the data from the tributaries can be better explained by a Ca isotope fractionation factor closer to unity, consistent with a surface runoff, probably with a short residence time (Fig. 6). On the other hand, the data from the mainstem of the Marsyandi (especially during the monsoon) requires the admixture of groundwater, characterised by an $\alpha^{Ca}_{water-calcite}$ of 1.0004, and also consistent with a longer hydrological pathway. With better constrained Mg and Ca isotope fractionation factors, not only the size but also the rate of incongruent dissolution could in future be quantified.

Although we advocate fractionation as the dominant control, the tributaries draining the LHS dolostones are strongly influenced by the isotopic composition of the source rock with high δ^{44}_{42}Ca values. Ca isotope ratios may prove useful in quantifying Ca derived from these LHS rocks. This signature is clearly visible in relatively large basins such as the Andhi Khola (sample NH7) (400 km^2). It is, however, worth noting that the contribution of the weathering of these rocks is rather small to large Himalayan rivers, and the δ^{44}_{42}Ca values in the large Himalayan rivers presented here show no particular offset to elevated δ^{44}_{42}Ca values. This supports previous estimates of the surface area (4%) and contribution of these lithologies to riverine chemistry by Osmium isotopic compositions of the dissolved and bed load (Sharma et al., 1999; Pierson-Wickmann et al., 2002).

Our findings also have wider implications. Whilst the oceanic budget of Mg has recently been discussed in light of riverine Mg isotope compositions (Tipper et al.,

2006b), the modern Ca cycle remains relatively poorly quantified (Milliman, 1993) and Ca isotope ratios may have an application in better constraining the oceanic budget of Ca (e.g. De La Rocha and DePaolo, 2000; Fantle and DePaolo, 2005; Farkaš et al., 2006; Sime et al., 2007). As yet, there has been no systematic survey of Ca isotope ratios in global rivers, but the data presented here may give some insight into the $\delta^{\frac{44}{42}}$Ca value of continental runoff. At a global scale, about two thirds of riverine Ca is derived from carbonate weathering (Milliman, 1993; Berner and Berner, 1996). The average $\delta^{\frac{44}{42}}$Ca values of rivers draining limestone in the present study is 0.46‰, and is slightly elevated compared to the present estimate of the carbonate sink of Ca from the oceans at 0.30‰ (De La Rocha and DePaolo, 2000; Fantle and DePaolo, 2005, 2007). The mechanism proposed for the enrichment in the heavy isotopes of Ca for rivers draining limestone is the preferential uptake of the light isotopes of Ca by secondary calcite. A second mechanism shown here is the occurrence and congruent dissolution of Proterozoic dolomite. Basins with a greater surface area draining this rock type are anticipated to deliver a source of isotopically heavy Ca to the oceans. In addition, when all available Ca isotope analyses of river waters and bulk carbonates are compared (Fig. 7), the riverine Ca isotope ratios are marginally offset towards elevated Ca isotope ratios, compared to both bulk carbonate $\delta^{\frac{44}{42}}$Ca values. Although these differences in $\delta^{\frac{44}{42}}$ Ca values are small, they merit further investigation at a global scale to ascertain whether this is merely a sampling or analytical artifact or a true observation. In particular, great care should be taken to assess seasonal variations in the quantification of the riverine input to the oceans. Such variations have already been reported for the Marsyandi, and although small, the 0.25‰ difference in $\delta^{\frac{44}{42}}$Ca values between the dry season (Schmitt et al., 2003) and the monsoon period (this study) for the Ganges suggests that seasonal variations might be more widespread. If true, the apparently small 0.17‰ difference between riverine input and carbonate output from the oceans, has been demonstrated to have a significant impact to the modelling and interpretation of the oceanic Ca cycle through the Neogene (Sime et al., 2007), implying that either the modern marine Ca isotope budget is not at steady state or that the isotopic compositions of the sources and sinks of Ca remain insufficiently characterised.

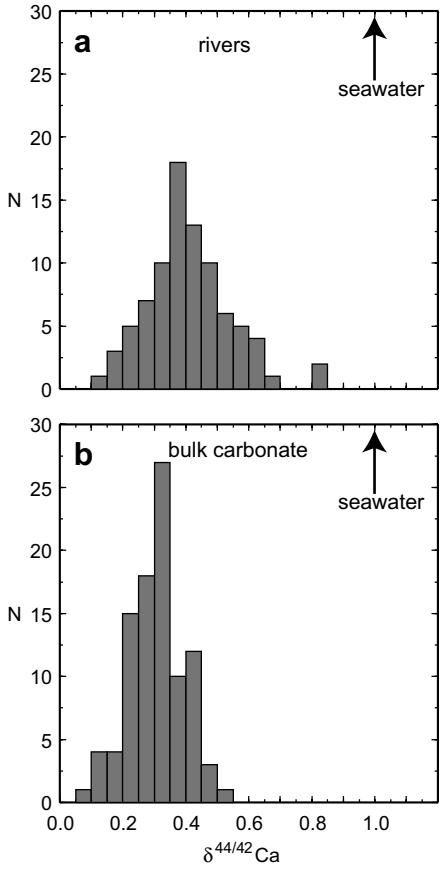

Fig. 7. Histograms of compilations of Ca isotope data in rivers. Data is from the present study, Schmitt et al. (2003), Zhu and Macdougall (1998) and Tipper et al. (2006a) for rivers, Fantle and DePaolo (2007), Fantle and DePaolo (2005) and De La Rocha and DePaolo (2000) for bulk carbonate.

7. CONCLUSIONS

Mg and Ca isotope ratios have been measured in both small and large rivers draining each of the major lithotectonic units from the Himalaya. The $^{26}Mg/^{24}Mg$ ratio shows a range of 2‰ and the $^{44}Ca/^{42}Ca$ ratio shows a range of 0.6‰, similar to the range identified between the principal rock reservoirs: limestone, dolostone and silicates. However, to a large extent the lithological control is obscured. For example, the average δ^{26}Mg value in tributaries draining predominantly mono-lithological catchments of limestone, dolostone and silicate rock is within the uncertainty of the method (0.14‰) in spite of a 2‰ range in the rock.

However in some cases, $\delta^{\frac{44}{42}}$Ca and δ^{26}Mg values may be used to infer the source of these elements at a small scale. In the dissolved load of tributaries draining the dolomitic LHS, δ^{26}Mg, $\delta^{\frac{44}{42}}$Ca and Mg/Ca values are indistinguishable from dolostone bedrock, suggesting a congruent dissolution of dolostone. These tributaries have the highest solute $\delta^{\frac{44}{42}}$Ca values reported so far, apart from seawater. In the TSS (limestone) and HHCS (silicate), where no dolomite is present, tributaries have similar δ^{26} Mg values in the solute phase, intermediate between limestone and silicate rock. Although this could result from a mixture between limestone and silicate derived Mg, it would be very surprising if Mg in tributaries draining two very different rock types, was derived in the same proportions from carbonate and silicate rock. Small rivers draining mainly silicate rock, have a mean δ^{26}Mg value which is on average 1.1‰ lower than silicate rock, consistent with previous reports of fractionation of Mg isotope ratios during silicate weathering. In the TSS, where Mg is a trace element in limestone, the δ^{26}Mg data implies that tributary Mg is strongly influenced by the small amounts of silicate mineral dissolution, whereas the source of Ca is overwhelmingly dominated by

carbonate dissolution. However, Ca isotope ratios of solute Ca are enriched in the heavy isotopes compared to bedrock $\delta^{\frac{44}{42}}$Ca values. Precipitation of secondary calcite, observed to be enriched in the light isotopes of Ca, is likely to be the main mechanism for this enrichment.

In spite of the strong gradient in vegetation density between the tributaries analysed, no systematic variations are observed in the Ca and Mg isotopic fractionation factors between rock and water. In particular, tributaries draining the densely vegetated LHS have both $\delta^{\frac{44}{42}}$Ca and δ^{26}Mg values similar to rock $\delta^{\frac{44}{42}}$Ca and δ^{26}Mg values. This preliminary result suggests that the cycling of Ca and Mg by vegetation cannot be resolved in Himalayan river waters using these isotope ratios.

Mg and Ca isotope ratios in rivers are therefore controlled by both heterogeneity in source rock Ca and Mg isotope ratios, and fractionation of Ca and Mg isotope ratios during the transfer of Ca and Mg from rock to the dissolved load. The interpretation of these isotope ratios in rivers is therefore complex, but will help improve current understanding of the origin of Ca and Mg and their path taken from rock to river. The fractionation of Ca and Mg isotope ratios during weathering implies that these elements are at least in part recycled during chemical alteration. Ca isotope ratios in rivers show a greater variability than previously acknowledged. Whether process related or lithology derived, there is a growing database of rivers draining carbonate rock with elevated $\delta^{\frac{44}{42}}$Ca values compared to modern marine limestone. The variability of Ca isotope ratios in modern rivers will need to be better constrained and accounted for in future models of global Ca cycling, if their extrapolation to the geological past is to have any significance.

ACKNOWLEDGMENTS

This research has been supported by the NERC. Edward Tipper was supported by a NERC studentship No. NER/S/A/2002/10342 and a CASE studentship from *Nu* Instruments. Katy Grant provided valuable support in the field. Samples labelled BR were analysed with the permission of Christian France-Lanord. John Becker collected samples M0316, M0308 and T0320 and the hot springs and provided the chemical data. Fatima Khan performed a large portion of the Sr isotope chemistry and Hazel Chapman performed the Sr isotope analyses by TIMS. Mervyn Greeves provided assistance with ICP-AES. Ian Wilshaw at The University of Keele, Caroline Gorge from IPGP and Graham Howell from the OU are thanked for anion analysis. Tank P. Ohja provided valuable logistical assistance in Nepal. Helpful discussions with Neil Sime, Jérôme Gaillardet, Josh West, Ed Carder and Damien Calmels greatly improved many of the ideas discussed in this manuscript. Clark Johnson is thanked for editorial handling and constructive comments. The comments of three anonymous reviewers substantially improved an earlier version of this manuscript.

APPENDIX A

See Tables A1–A3.

Table A1
Major cations and anions and Sr isotope data for river water samples

Sample	Location	Date	*N* (deg)	*E* (deg)	*T*	pH	Ca (μmol/l)	K (μmol/l)	Mg (μmol/l)	Na (μmol/l)	$Si(OH)_4$ (μmol/l)	Sr (μmol/l)	Cl^- (μmol/l)	SO_4^{2-} (μmol/l)	HCO_3^- (μmol/l)	$^{87}Sr/^{86}Sr$	TDS (mg/l)	SI_{cc}
TSS rivers																		
ett7	Marsyandi	06-Sep	28.574	84.173	14.1	7.73	1151	51	251	155	104	2.77	97	269	2360	0.71640	237	1.00
ett8	Marsyandi	06-Sep	28.592	84.198	na	na	1749	86	1617	104	116	4.84	17	1275	4355	na	512	na
ett9	Marsyandi	06-Sep	28.604	84.166	11.7	6.65	1674	27	208	39	71	1.24	7	105	3578	na	310	0.18
ett10	Marsyandi	06-Sep	28.606	84.163	11.9	8.28	499	6	127	26	50	0.45	10	71	1130	na	103	0.94
ett11	Marsyandi	06-Sep	28.608	84.158	12.6	8.34	1090	43	413	124	119	2.46	247	249	2424	0.72477	245	1.51
ett12[a]	Marsyandi	06-Sep	28.611	84.155	9.3	8.65	667	59	173	21	22	0.75	10	168	1408	0.72431	138	1.39
ett13	Marsyandi	06-Sep	28.617	84.147	9.6	8.46	818	19	276	23	30	1.50	17	306	1597	0.72630	171	1.36
ett14[a]	Marsyandi	07-Sep	28.620	84.138	13.4	8.32	1284	20	618	119	129	2.96	15	439	3040	0.73103	306	1.62
ett16[a]	Marsyandi	07-Sep	28.632	84.114	10.4	8.51	1177	19	203	32	52	1.37	18	193	2402	0.73057	223	1.66
ett17[a]	Marsyandi	07-Sep	28.633	84.107	11.8	8.57	1687	8	766	20	46	1.84	9	1299	2324	0.71936	358	1.84
ett18[a]	Marsyandi	07-Sep	28.637	84.092	12.4	8.60	1336	21	765	30	43	2.40	8	845	2550	0.71881	315	1.80
ett19	Marsyandi	07-Sep	28.640	84.087	19.2	8.34	1212	12	229	41	81	2.53	9	131	2663	0.71376	236	1.65
ett20	Marsyandi	07-Sep	28.645	84.070	11.4	8.49	838	23	516	37	33	2.21	11	465	1820	0.71702	207	1.44
ett21	Marsyandi	07-Sep	28.648	84.048	7.0	8.09	795	10	273	18	23	1.21	7	380	1392	0.72766	163	0.95
ett23[a]	Marsyandi	08-Sep	28.663	84.028	8.7	8.26	1396	18	732	294	68	0.06	8	1179	2189	0.71722	333	1.46
ett24[a]	Marsyandi	08-Sep	28.657	84.039	16.0	8.10	1407	17	1576	201	135	5.51	16	966	4233	0.72256	460	1.56
ett25	Marsyandi	08-Sep	28.651	84.034	9.8	8.14	906	7	288	21	42	0.94	7	264	1875	0.72534	188	1.17
ett26	Marsyandi	08-Sep	28.654	84.032	9.8	8.46	780	7	253	15	25	0.93	5	295	1486	0.72352	160	1.32
ett27	Marsyandi	08-Sep	28.659	84.028	17.4	8.55	912	27	1173	86	90	2.42	8	550	3168	0.72605	321	1.69
ett28[a]	Marsyandi	08-Sep	28.664	84.018	6.0	8.40	723	20	275	18	22	1.62	4	412	1203	0.72477	152	1.13
ett29[a]	Marsyandi	08-Sep	28.670	84.018	11.7	8.58	1573	18	683	146	57	4.94	7	1244	2171	0.71824	340	1.81
ett30[a]	Marsyandi	09-Sep	28.668	84.004	6.8	8.53	934	31	589	93	43	2.62	6	663	1832	0.72266	234	1.46
ett33	Marsyandi	10-Sep	28.691	83.993	9.7	7.60	1634	13	492	292	142	0.07	12	659	3222	0.71371	352	1.04
ett34[a]	Marsyandi	10-Sep	28.700	83.991	7.2	8.67	1500	21	660	305	49	6.06	10	1140	2348	0.71478	341	1.82
ett35	Marsyandi	10-Sep	28.718	83.977	8.9	8.48	1410	11	265	147	95	3.96	6	515	2466	0.71779	272	1.70
ett36	Marsyandi	10-Sep	28.722	83.974	7.1	8.90	1380	7	243	94	72	3.79	6	624	2082	0.71289	256	1.93
ett37	Marsyandi	10-Sep	28.726	83.889	8.9	8.39	1296	11	347	224	125	3.99	9	460	2576	0.71487	275	1.60
ett38	Marsyandi	10-Sep	28.737	83.974	4.8	8.30	1406	25	661	382	50	5.49	6	1120	2288	0.71503	334	1.46
ett39	Marsyandi	10-Sep	28.740	83.974	6.7	8.37	1048	12	589	44	47	2.69	97	610	2006	0.71248	246	1.40
ett40	Marsyandi	11-Sep	28.742	83.973	7.9	8.27	766	5	97	52	71	1.04	6	63	1627	0.71444	145	1.16
ett41	Marsyandi	11-Sep	28.747	83.971	6.5	7.90	1176	22	518	124	76	4.15	7	427	2657	0.71649	273	1.10
ett42	Marsyandi	11-Sep	28.777	83.977	4.6	8.51	1825	26	824	86	29	4.47	9	1538	2321	0.71206	389	1.75
ett44	Marsyandi	11-Sep	28.732	83.966	7.2	8.24	1704	23	878	145	70	6.80	7	1297	2720	na	390	0.61
ett45	Marsyandi	11-Sep	28.757	83.965	6.7	8.56	1575	24	819	173	56	7.43	9	1496	1970	0.71673	357	0.73
ett46	Marsyandi	11-Sep	28.762	83.966	9.2	8.36	1734	8.9	435	173	70	5.29	8	585	3325	0.71480	350	0.88
ett50	Marsyandi	13-Sep	28.650	84.083	8.3	8.70	1431	19	1069	130	64	4.34	10	1200	2735	0.72918	374	0.98
ett53	Marsyandi	13-Sep	28.651	84.099	11.9	8.55	1258	17	679	66	67	2.49	9	838	2261	0.72473	293	0.80
ett54	Marsyandi	13-Sep	28.648	84.105	12.0	8.35	1398	17	512	56	70	2.61	10	994	1882	0.72981	286	0.57
ett56	Marsyandi	13-Sep	28.644	84.123	na	na	944	23	502	58	108	1.50	8	113	2730	0.72741	236	na
ett58	Marsyandi	13-Sep	28.639	84.131	11.9	8.69	690	19	859	28	62	2.12	10	425	2267	0.72172	234	0.69
ett59	Marsyandi	13-Sep	28.635	84.136	11.4	8.58	666	6.8	917	17	50	2.12	9	598	1973	0.71410	232	0.51
ett61[a]	Marsyandi	14-Sep	28.612	84.163	8.5	8.57	760	13	810	21	47	2.13	7	602	1954	0.71295	232	0.51
ett63[a]	Marsyandi	14-Sep	28.571	84.186	na	na	720	24	121	16	27	1.21	na	na	1723	0.71438	141	na
ett65	Marsyandi	14-Sep	28.565	84.219	13.4	8.12	1153	41	89	31	80	1.04	15	137	2245	0.71671	207	0.43
ett69[a]	Marsyandi	14-Sep	28.554	84.259	12.2	8.47	947	29	457	104	45	2.67	36	647	1604	0.71860	217	0.49
ett74[a]	Nar	15-Sep	28.555	84.259	12.7	8.49	1437	28	834	163	49	5.19	33	1359	1973	0.71443	339	0.72
MT2[a]	Nar	01-Aug	28.555	84.259	na	na	897	27	337	102	25	2.49	16	579	1426	0.71000	192	na
MT113[a]	Nar	24-Dec	28.555	84.259	na	na	1211	34	916	209	77	4.96	36	1316	1843	0.72000	318	na
ace68	Arun	21-Aug	28.619	86.474	11.8	8.36	1164	24	343	238	110	3.45	22	595	1826	0.71055	235	1.48

SI_{cc} is the calcite saturation index calculated using PHREEQC.

[a] Data already published in Tipper et al. (2006c).

Table A2
Major cations and anions and Sr isotope data for river water samples

Sample	Location	Date	*N* (deg)	*E* (deg)	*T*	pH	Ca (μmol/l)	K (μmol/l)	Mg (μmol/l)	Na (μmol/l)	$Si(OH)_4$ (μmol/l)	Sr (μmol/l)	Cl^- (μmol/l)	SO_4^{2-} (μmol/l)	HCO_3^- (μmol/l)	$^{87}Sr/^{86}Sr$	TDS (mg/l)	SI_{cc}
HHCS rivers																		
ett4	Marsyandi	04-Sep	28.411	84.406	20.0	7.25	86	34	26	69	195	0.13	15	28	249	na	32	−2.31
ett5	Marsyandi	04-Sep	28.427	84.395	15.7	6.74	83	30	24	103	298	0.16	82	111	33	na	32	-3.79
ett6	Marsyandi	04-Sep	28.472	84.376	17.0	8.18	409	16	21	32	117	0.28	11	35	817	na	77	−0.28
ett66	Marsyandi	14-Sep	28.552	84.242	11.0	8.35	544	16	18	19	52	0.32	24	74	978	na	94	−0.02
ett67	Marsyandi	14-Sep	28.551	84.244	11.5	8.22	421	11	15	17	55	0.17	4	56	779	0.72676	74	−0.33
ett68	Marsyandi	14-Sep	28.554	84.259	9.8	8.21	345	14	20	26	77	0.17	9	41	671	na	64	−0.51
ett70	Marsyandi	15-Sep	28.594	84.241	9.8	8.42	829	27	103	23	58	0.80	12	274	1345	0.71926	150	0.31
ett73	Marsyandi	15-Sep	28.551	84.258	13.3	8.18	793	32	161	25	78	0.67	12	49	1839	na	160	0.26
ett75	Marsyandi	16-Sep	28.551	84.265	12.4	8.04	290	11	17	18	55	0.17	7	13	595	na	54	−0.76
ett76	Marsyandi	16-Sep	28.543	84.289	10.7	8.02	249	14	14	25	71	0.13	3	30	492	0.72882	47	−0.95
ett78	Marsyandi	16-Sep	28.528	84.304	13.3	7.83	259	17	17	38	102	0.17	6	42	501	na	51	−1.07
ett79	Marsyandi	16-Sep	28.526	84.312	12.2	8.24	419	19	18	28	64	0.30	8	77	751	0.72263	75	−0.32
ett81	Marsyandi	16-Sep	na	na	12.6	8.27	404	20	16	21	65	0.31	26	54	735	0.72086	72	−0.31
ett83	Marsyandi	16-Sep	28.535	84.334	14.4	8.54	331	14	24	65	83	0.27	53	46	635	0.72446	64	−0.17
ett84	Marsyandi	16-Sep	28.537	84.327	13.0	8.95	1044	27	544	130	52	3.24	43	867	1549	na	242	0.94
ett85	Marsyandi	16-Sep	28.533	84.339	13.6	7.53	661	37	41	31	137	0.45	10	62	1309	na	123	−0.59
ett87	Marsyandi	17-Sep	28.545	84.376	13.7	8.17	328	11	41	35	97	0.27	9	35	696	na	65	−0.50
ett88	Marsyandi	17-Sep	28.559	84.395	13.9	8.02	299	10	33	62	111	0.23	26	36	629	na	62	−0.72
ett89	Marsyandi	17-Sep	28.569	84.405	11.3	8.19	417	15	35	46	97	0.30	25	58	813	0.72129	79	−0.35
ett91	Marsyandi	17-Sep	0.000	0.000	10.9	8.25	920	40	69	47	126	0.75	12	129	1765	na	169	0.33
ett92	Marsyandi	17-Sep	28.541	84.375	10.0	8	954	47	93	43	160	0.72	11	144	1842	na	179	0.10
ett93	Marsyandi	17-Sep	na	na	11.2	8.44	955	50	79	39	175	0.74	12	131	1848	na	178	0.55
ett95	Marsyandi	17-Sep	na	na	11.6	8.2	491	19	27	30	66	0.59	11	78	909	0.72072	88	−0.23
ett96	Marsyandi	17-Sep	28.527	84.358	10.5	8.26	435	14	36	60	78	0.39	38	64	842	0.72632	83	−0.27
ett97	Marsyandi	18-Sep	28.504	84.360	12.3	8.19	757	35	44	43	152	0.59	11	62	1525	na	140	0.16
ett98	Marsyandi	18-Sep	28.502	84.360	14.2	7.97	561	22	30	36	125	0.40	7	69	1085	na	103	−0.29
ett99	Marsyandi	18-Sep	28.498	84.361	10.2	8.54	628	23	32	33	147	0.41	13	36	1276	na	116	0.32
ett101	Marsyandi	18-Sep	28.495	84.362	10.0	8.43	438	15	20	18	92	0.26	11	15	899	na	80	−0.07
ett103	Marsyandi	18-Sep	28.491	84.363	6.8	8.39	423	35	28	63	160	0.36	9	77	813	na	85	−0.23
ett104	Marsyandi	18-Sep	28.490	84.366	6.3	7.98	108	16	23	58	146	0.13	42	43	202	na	30	−1.79
ett105	Marsyandi	18-Sep	na	na	6.1	8.47	735	32	48	47	192	0.52	16	31	1539	na	139	0.33
ett107	Marsyandi	18-Sep	28.464	84.372	6.9	7.5	790	25	303	127	66	1.94	431	36	1823	na	177	−0.53
ett109	Marsyandi	18-Sep	28.448	84.378	12.9	6.73	94	39	19	628	203	0.84	481	36	336	0.75558	68	−2.79
ett110	Marsyandi	18-Sep	28.443	84.383	13.3	6.73	99	48	25	863	246	0.83	10	51	1039	0.75528	103	−2.29
ett111	Marsyandi	18-Sep	28.427	84.398	14.2	7.74	91	38	27	89	282	0.17	21	68	200	na	36	−1.98
ett112	Marsyandi	19-Sep	28.418	84.404	13.8	7.52	121	48	29	122	242	0.15	0	0	470	na	46	−1.71
ett114	Marsyandi	19-Sep	28.407	84.407	15.5	8.3	73	31	25	88	237	0.17	23	11	268	na	32	−1.37
ett118	Marsyandi	19-Sep	28.398	84.407	15.9	7.27	106	35	30	87	259	0.18	8	41	302	na	39	−2.18
ett119	Marsyandi	19-Sep	28.395	84.408	13.0	7.3	111	31	24	107	257	0.21	7	36	328	na	40	−2.14
ett121	Marsyandi	19-Sep	28.393	84.404	14.0	7.49	103	25	22	95	239	0.20	2	30	308	na	37	−1.99
ett123	Marsyandi	19-Sep	28.386	84.402	12.0	7.07	47	14	14	48	169	0.09	4	24	125	na	19	-3.16
ett125	Marsyandi	19-Sep	28.371	84.406	14.2	7.58	115	46	37	98	174	0.32	47	40	309	0.74042	40	−1.86
ett126	Marsyandi	19-Sep	28.369	84.406	15.4	7.8	170	51	44	145	303	0.31	18	34	532	na	59	−1.23
ett131	Marsyandi	19-Sep	28.364	84.406	13.2	7.45	77	24	27	64	174	0.16	6	48	190	na	28	−2.37
ett132	Marsyandi	19-Sep	na	na	8.0	8.1	731	37	259	193	85	1.72	157	409	1226	0.72043	165	−0.13
ett134	Marsyandi	19-Sep	28.354	84.407	15.5	7.15	58	42	36	80	206	0.10	33	75	125	0.75003	29	−2.95
ett135	Marsyandi	19-Sep	28.352	84.408	15.4	7.15	46	33	33	74	205	0.08	7	46	164	na	26	−2.93
M0308	Marsyandi	20-Oct	28.352	84.408	16.4	7.02	50	41	41	101	225	0.10	9	50	227	0.74893	16	−1.74
M0316	Marsyandi	21-Oct	28.427	84.398	16.7	7.02	88	40	28	103	265	0.20	18	57	247	0.73702	18	−1.46

SI_{cc} is the calcite saturation index calculated using PHREEQC.

Table A3
Major cations and anions and Sr isotope data for river water samples

Sample	Location	Date	*N* (deg)	*E* (deg)	*T*	pH	Ca (μmol/l)	K (μmol/l)	Mg (μmol/l)	Na (μmol/l)	$Si(OH)_4$ (μmol/l)	Sr (μmol/l)	Cl^- (μmol/l)	SO_4^{2-} (μmol/l)	HCO_3^- (μmol/l)	$^{87}Sr/^{86}Sr$	TDS (mg/l)	SI_{cc}
LHS rivers																		
ett2	Marsyandi	03-Sep	28.310	84.401	22.7	8.50	869	93	521	53	131	0.20	15	111	2676	0.85058	234	0.85
ett3	Marsyandi	03-Sep	28.316	84.410	19.2	7.45	327	25	40	105	117	0.31	43	71	673	na	71	−1.15
ett136	Marsyandi	19-Sep	28.342	84.407	16.5	8.40	492	64	89	108	239	0.45	117	28	1160	0.72394	112	0.14
ett138	Marsyandi	20-Sep	28.336	84.408	17.0	8.36	1205	93	154	161	123	0.89	10	69	2822	na	245	0.81
ett139	Marsyandi	20-Sep	28.333	84.404	18.7	8.62	1718	61	168	117	341	0.98	25	24	3872	na	331	1.33
ett142	Marsyandi	20-Sep	28.321	84.402	19.8	8.34	1338	65	124	80	533	0.99	20	53	2898	na	264	0.89
ett147	Marsyandi	20-Sep	28.313	84.403	16.8	8.47	1167	100	600	79	221	0.47	16	60	3576	na	301	0.98
ett148	Marsyandi	20-Sep	28.313	84.403	22.5	9.10	1235	135	663	100	235	0.46	14	246	3524	na	322	1.56
ett149	Marsyandi	20-Sep	28.301	84.389	21.2	8.33	823	87	672	69	177	0.25	9	174	2775	0.80905	249	0.66
ett150	Marsyandi	20-Sep	28.299	84.387	21.3	8.32	931	105	922	79	211	0.27	13	38	3793	0.79202	311	0.82
ett151	Marsyandi	20-Sep	28.298	84.385	21.1	8.13	852	109	842	72	199	0.23	8	28	3494	0.80839	286	0.58
ett153	Marsyandi	20-Sep	28.293	84.379	22.0	7.61	900	136	830	132	262	0.46	14	387	2939	0.84413	292	0.02
ett154	Marsyandi	20-Sep	28.292	84.376	22.0	7.95	902	102	623	84	178	0.27	15	253	2692	na	255	0.33
ett156	Marsyandi	21-Sep	28.288	84.363	16.8	8.22	1017	101	587	89	215	0.33	13	144	3096	0.81220	273	0.63
ett157	Marsyandi	21-Sep	28.280	84.357	9.5	7.88	254	40	103	62	146	0.15	10	62	675	na	68	−0.97
ett158	Marsyandi	21-Sep	28.265	84.364	25.0	8.38	373	41	186	64	152	0.17	8	32	1151	na	101	0.12
ett160	Marsyandi	21-Sep	28.251	84.371	25.7	8.36	270	23	47	80	161	0.22	19	15	686	na	64	−0.23
ett161	Marsyandi	21-Sep	28.239	84.373	27.3	7.67	109	31	32	85	169	0.13	32	20	320	na	36	−1.58
ett162	Marsyandi	22-Sep	28.223	84.380	22.4	7.70	107	20	29	81	166	0.15	16	11	327	0.78336	35	−1.62
ett163	Marsyandi	22-Sep	28.111	84.428	22.5	7.47	107	24	37	125	196	0.22	26	10	383	na	41	−1.78
ett155	Marsyandi	21-Sep	28.289	84.364	14.0	8.05	715	40	249	202	98	1.59	164	373	1251	0.72189	163	−0.09
ett164	Trisuli	22-Sep	27.871	84.608	19.0	8.18	406	33	147	113	136	0.60	23	124	970	0.73646	101	−0.20
ct59	Marsyandi	07-May	28.301	24.760	21.1	8.11	1006	109	893	87	190	0.32	7.41	7.55	3290	0.80954	306	1.43
Marsyandi main river																		
ett1	Marsyandi	02-Sep	27.954	84.424	22.5	7.86	548	33	185	133	128	1.02	68	218	1117	0.72325	127.52	0.72
ett22[a]	Marsyandi	07-Sep	28.664	84.021	8.7	8.45	1147	31	608	132	39	3.55	17	941	1766	0.71757	267	1.49
ett43[a]	Marsyandi	11-Sep	28.777	83.977	5.6	8.51	1727	25	988	131	34	5.33	9	1651	2268	0.71145	398	0.76
ett69[a]	Marsyandi	14-Sep	28.554	84.259	12.2	8.47	947	29	457	104	45	2.67	36	647	1604	0.71860	217	0.49
ett84	Marsyandi	16-Sep	28.537	84.327	13.0	8.95	1044	27	544	130	52	3.24	43	867	1549	na	242	0.94
ett107	Marsyandi	18-Sep	28.464	84.372	6.9	7.50	790	25	303	127	66	1.94	431	36	1823	na	177	−0.53
ett132	Marsyandi	19-Sep	na	na	8.0	8.10	731	37	259	193	85	1.72	157	409	1226	0.72043	165	−0.13
ett155	Marsyandi	21-Sep	28.289	84.364	14.0	8.05	715	40	249	202	98	1.59	164	373	1251	0.72189	163	−0.09
T0320	Trisuli	07-Nov	28.210	85.549	4.5	7.10	257	24	38	104	81	0.30	0	0	526	0.75531	23	−0.83
Hot springs																		
HS7[b]	Marsyandi	04-May	28.531	84.350	34.0	na	8549	3447	798	28512	1746	45	46486	299	3092	na	3018	na
HS9[b]	Marsyandi	14-May	28.340	84.398	50.0	na	21650	12005	4304	75762	1588	120	117018	1232	17146	0.76945	8497	na

SI_{cc} is the calcite saturation index calculated using PHREEQC.
[a] Data already published in Tipper et al. (2006c).
[b] Data from Becker (2005).

REFERENCES

Becker, J. A. (2005) Quantification of Himalayan Metamorphic CO_2 fluxes: impact on Global Carbon Budgets. Ph.D. Thesis, Department of Earth Sciences, University of Cambridge, Downing St., Cambridge, CB2 3EQ.

Berner E. K. and Berner R. A. (1996) *Global Environment: Water, Air, and Geochemical Cycles*. Prentice Hall, Upper Saddle River, N.J.

Berner R. A., Lasaga A. C. and Garrels R. M. (1983) The carbonate–silicate geochemical cycle and its effect on atmospheric carbon dioxide over the past 100 million years. *Am. J. Sci.* **283**, 641–683.

Bickle M. J., Bunbury J., Chapman H. J., Harris N. B. W., Fairchild I. and Ahmad T. (2001) Controls on the Sr ratio of carbonates in the Garhwal Himalaya, Headwaters of the Ganges. *J. Geol.* **109**, 737–753.

Bickle M. J., Bunbury J., Chapman H. J., Harris N. B. W., Fairchild I. and Ahmad T. (2003) Fluxes of Sr into the Headwaters of the Ganges. *Geochim. Cosmochim. Acta* **67**, 2567–2584. doi:10.1016/S0016-7037(03)00029-2.

Bickle M. J., Chapman H. J., Bunbury J., Harris N. B. W., Fairchild I. J., Ahmad T. and Pomiès C. (2005) Relative contributions of silicate and carbonate rocks to riverine Sr fluxes in the headwaters of the Ganges. *Geochim. Cosmochim. Acta* **69**, 2221–2240. doi:10.1016/j.gca.2004.11.019.

Black J. R., Yin Q. Z. and Casey W. H. (2006) An experimental study of magnesium-isotope fractionation in chlorophyll-a. *Geochim. Cosmochim. Acta* **70**, 4072–4079. doi:10.1016/j.gca.2006.06.010.

Blum J. D., Carey A. G., Jacobson A. D. and Chamberlain P. (1998) Carbonate versus silicate weathering in the Raikhot watershed within the High Himalayan Crystalline Series. *Geology* **26**, 411–414.

Bordet P., Colchen M., Krummenacher D., Lefort P., Mouterde R., Remy M. (1971) *Recherches Geologiques dans l'Himalaya du Nepal region de la Thakkhola*. Editions du centre national de la recherche scientifique.

Burbank D., Blythe A., Putkonen J., Pratt-Sitaula B., Gabet E., Oskin M., Barros A. and Ojha T. (2003) Decoupling of erosion and precipitation in the Himalayas. *Nature* **426**, 652–655.

Carder E. A., Galy A. and Elderfield H. (2004) The magnesium isotopic composition of oceanic water masses. *Geochim. Cosmochim. Acta* **68**, A329.

Chabaux F., Riotte J., Clauer N. and France-Lanord C. (2001) Isotopic tracing of the dissolved U fluxes of Himalayan rivers: implications for present and past U budgets of the Ganges–Brahmaputra system. *Geochim. Cosmochim. Acta* **65**, 3201–3217. doi:10.1016/S0016-7037(01)00669-X.

Chang V. T. C., Makishima A., Belshaw N. S. and O'Nions R. K. (2003) Purification of Mg from low Mg biogenic carbonates for isotope ratio determination using multiple collector ICP-MS. *J. Anal. Atom. Spectrom.* **18**, 296–301.

Colchen M., Le Fort P., Pecher A. (1986) *Notice explicative de la Carte Geologique Annapurna–Manaslu–Ganesh (Himalaya du Nepal) au 1:200.000e*. Centre National de la recherche Scientifique.

De La Rocha C. L. and DePaolo D. J. (2000) Isotopic evidence for variations in the marine calcium cycle over the Cenozoic. *Science* **289**, 1176–1178.

DePaolo D. J. (2004) Calcium isotopic variations produced by biological, kinetic, radiogenic and nucleosyntheitic processes. *Rev. Min. Geochem.* **55**, 255–288.

Derry L. A., Kurtz A. C., Ziegler K. and Chadwick O. A. (2005) Biological control of terrestrial silica cycling and export fluxes to watersheds. *Nature* **433**, 728–731.

Drever J. I. (1994) The effect of land plants on weathering rates of silicate minerals. *Geochim. Cosmochim. Acta* **58**, 2325–2332.

Edmond J. M. (1992) Himalayan tectonics, weathering processes, and the strontium isotope record in marine limestones. *Science* **258**, 1594–1597.

Eisenhauer A., Nägler T. F., Stille P., Kramers J., Gussone N., Bock B., Fietzke J., Hippler D. and Schmitt A. D. (2004) Proposal for international agreement on Ca notation resulting from discussions at workshops on stable isotope measurements held in Davos (Goldschmidt 2002) and Nice (EGS-AGU-EUG 2003). *Geostand. Geoanal. Res.* **28**, 149–151.

English N., Quade J., DeCelles P. and Garzione C. (2000) Geologic control of Sr and major element chemistry in Himalayan Rivers, Nepal. *Geochim. Cosmochim. Acta* **64**, 2549–2566.

Evans M. J., Derry L. A., Anderson S. and France-Lanord C. (2001) Hydrothermal source of radiogenic Sr to Himalayan rivers. *Geology* **29**, 803–806.

Evans M. J., Derry L. A. and France-Lanord C. (2004) Geothermal fluxes of alkalinity in the Narayani river system of central Nepal. *Geochem. Geophys. Geosyst.* **5**, Q08011.

Fantle M. S. and DePaolo D. J. (2005) Variations in the marine Ca cycle over the past 20 million years. *Earth Planet. Sci. Lett.* **237**, 102–117. doi:10.1016/j.epsl.2005.06.024.

Fantle M. S. and DePaolo D. J. (2007) Ca isotopes in carbonate sediment and pore fluid from ODP Site 807A: the Ca^{2+}(aq) calcite equilibrium fractionation factor and calcite recrystallization rates in Pleistocene sediments. *Geochim. Cosmochim. Acta* **71**, 2524–2546. doi:10.1016/j.gca.2007.03.006.

Farkaš J., Buhl D., Blenkinsop J. and Veizer J. (2006) Evolution of the oceanic calcium cycle during the late Mesozoic: evidence from $\delta^{44/40}$Ca of marine skeletal carbonates. *Earth Planet. Sci. Lett.* **253**, 96–111. doi:10.1016/j.epsl.2006.10.015.

France-Lanord C., Evans M., Hurtrez J. E. and Riotte J. (2003) Annual dissolved fluxes from Central Nepal rivers: budget of chemical erosion in the Himalayas. *C. R. Geosci.* **335**, 1131–1140.

Gaillardet J., Dupré B., Louvat P. and Allègre C. J. (1999) Global silicate weathering and CO_2 consumption rates deduced from the chemistry of large rivers. *Chem. Geol.* **159**, 3–30.

Galy A., Bar-Mathews M., Halicz L. and O'Nions R. K. (2002) Mg isotopic composition of carbonate: insight from speleothem formation. *Earth Planet. Sci. Lett.* **201**, 105–115. doi:10.1016/S0012-821X(02)00675-1.

Galy A., Belshaw N., Halicz L. and O'Nions R. (2001) High-precision measurement of magnesium isotopes by multiple-collector inductively coupled plasma mass spectrometry. *Int. J. Mass Spectrom.* **208**, 89–98.

Galy A. and France-Lanord C. (1999) Weathering processes in the Ganges–Brahmaputra basin and the riverine alkalinity budget. *Chem. Geol.* **159**, 31–60. doi:10.1016/S0009-2541(99)00033-9.

Galy A., France-Lanord C. and Derry L. A. (1999) The strontium isotopic budget of Himalayan Rivers in Nepal and Bangladesh. *Geochim. Cosmochim. Acta* **63**, 1905–1925. doi:10.1016/S0016-7037(99)00081-2.

Galy A., Yoffe O., Janney P., Williams R., Cloquet C., Alard O., Halicz L., Wadhwa M., Hutcheon I., Ramon E. and Carignan J. (2003) Magnesium isotope heterogeneity of the isotopic standard SRM980 and new reference materials for magnesium-isotope-ratio measurements. *J. Anal. Atom. Spectrom.* **18**, 1352–1356.

Halicz L., Galy A., Belshaw N. S. and O'Nions R. K. (1999) High-precision measurement of calcium isotopes in carbonates and related materials by multiple collector inductively coupled plasma mass spectrometry (MC-ICP-MS). *J. Anal. Atom. Spectrosc.* **14**, 1835–1838.

Harris N., Bickle M. J., Chapman H., Fairchild I. and Bunbury J. (1998) The significance of Himalayan rivers for silicate weath-

ering rates: evidence from the Bhote Kosi tributary. *Chem. Geol.* **144**, 205–220.

Harris N., Vance D. and Ayres M. (1999) From sediment to granite: timescales of anatexis in the upper crust. *Chem. Geol.* **162**, 155–167.

Hippler D., Schmitt A., Gussone N., Heuser A., Stille P., Eisenhauer A. and Nägler T. (2003) Ca isotopic composition of various standards and seawater. *Geostand. Newslett.* **27**, 13–19.

Jacobson A. D. and Blum J. D. (2000) Ca/Sr and $^{87}Sr/^{86}Sr$ geochemistry of disseminated calcite in Himalayan silicate rocks from the Naga Parbat: influence on river water chemistry. *Geology* **28**, 463–466.

Jacobson A. D., Blum J. D. and Walter L. M. (2002) Reconciling the elemental and Sr isotope composition of Himalayan weathering fluxes: Insights from the carbonate geochemistry of stream waters. *Geochim. Cosmochim. Acta* **66**, 3417–3429.

Kisakurek B., James R. H. and Harris N. B. W. (2005) Li and δ^7Li in Himalayan rivers: proxies for silicate weathering? *Earth Planet. Sci. Lett.* **237**, 387–401.

Krishnaswami S., Trivedi J., Sarin M., Ramesh R. and Sharma K. (1992) Strontium isotopes and rubidium in the Ganga–Brahmaputra river system: weathering in the Himalaya, fluxes to the Bay of Bengal and contributions to the evolution of oceanic Sr. *Earth Planet. Sci. Lett.* **109**, 243–253.

Le Fort P. (1975) Himalayas, the collided range, present knowledge of the continental arc. *Am. J. Sci.* **275A**, 1–44.

Lemarchand D., Wasserburg G. and Papanastassiou D. (2004) Rate-controlled calcium isotope fractionation in synthetic calcite. *Geochim. Cosmochim. Acta* **68**, 4665–4678.

Milliman J. (1993) Production and accumulation of calcium carbonate in the ocean: budget of a nonsteady state. *Global Biogeochem. Cycles* **7**, 927–957.

Moulton K. L. and Berner R. A. (1998) Quantification of the effect of plants on weathering; studies in Iceland. *Geology* **26**, 895–898.

Moulton K. L., West J. and Berner R. A. (2000) Solute flux and mineral mass balance approaches to the quantification of plant effects on silicate weathering. *Am. J. Sci.* **300**, 539–570.

Oliver L., Harris N., Bickle M., Chapman H., Dise N. and Horstwood M. (2003) Silicate weathering rates decoupled from the ^{87}Sr ratio of the dissolved load during Himalayan erosion. *Chem. Geol.* **201**, 119–139.

Palmer M. R. and Edmond J. M. (1992) Controls over the strontium isotope composition of river water. *Earth Planet. Sci. Lett.* **56**, 2099–2111.

Pande K., Sarin M., Trivedi J., Krishnaswami S. and Sharma K. (1994) The Indus River system (India Pakistan): major-ion chemistry, uranium and Sr isotopes. *Chem. Geol.* **116**, 245–259.

Pierson-Wickmann A. C., Reisberg L. and France-Lanord C. (2002) Behavior of Re and Os during low-temperature alteration: Results from Himalayan soils and altered black shales. *Geochim. Cosmochim. Acta* **66**, 1539–1548.

Pratt-Sitaula B., Burbank D. W., Heimsath A. and Ohja T. (2004) Landscape disequilibrium on 100–10,000 year scales Marsyandi River, Nepal, Central Himalaya. *Geomorphology* **58**, 223–241.

Quade J., English N. and DeCelles P. G. (2003) Silicate versus carbonate weathering in the Himalaya: a comparison of the Arun and Seti River watersheds. *Chem. Geol.* **202**, 276–296.

Quade J., Roe L., DeCelles P. G. and Ojha T. P. (1997) The late Neogene $^{87}Sr/^{86}Sr$ record of lowland Himalayan rivers. *Science* **276**, 1826.

Raymo M. E., Ruddiman W. F. and Froelich P. N. (1988) Influence of late Cenozoic mountain building on ocean geochemical cycles. *Geology* **16**, 649–653.

Richter F. M., Rowley D. B. and DePaolo D. J. (1992) Sr isotope evolution of seawater: the role of tectonics. *Earth Planet. Sci. Lett.* **109**, 11–23.

Schmitt A. D., Chabaux F. and Stille P. (2003) The calcium riverine and hydrothermal isotopic fluxes and the oceanic calcium mass balance. *Earth Planet. Sci. Lett.* **213**, 503–518.

Schneider C. and Masch L. (1993) The metamorphism of the Tibetan Series from the Manang area, Marsyandi Valley, Central Nepal. *Geol. Soc. London Spec. Pub.*, 357–374.

Sharma M., Wasserburg G. J., Hofmann A. W. and Chakrapani G. J. (1999) Himalayan uplift and osmium isotopes in oceans and rivers. *GCA* **63**, 4005–4012. doi:10.1016/S0016-7037(99)00305-1.

Sime N. G., De La Rocha C. L. and Galy A. (2005) Negligible temperature dependence of calcium isotope fractionation in twelve species of planktonic foramifera. *Earth Planet. Sci. Lett.* **232**, 51–66. doi:10.1016/j.epsl.2005.01.011.

Sime N. G., De La Rocha C. L., Tipper E. T., Tripati A., Galy A. and Bickle M. J. (2007) Interpreting the Ca isotope record of marine biogenic carbonates. *Geochim. Cosmochim. Acta* **71**, 3979–3989. doi:10.1016/j.gca.2007.06.009.

Singh S. K., Trivedi J. R., Pande K., Ramesh R. and Krishnaswami S. (1998) Chemical and strontium, oxygen, and carbon isotopic compositions of carbonates from the Lesser Himalaya: implications to the strontium isotope composition of the source waters of the Ganga, Ghaghara, and the Indus rivers. *Geochim. Cosmochim. Acta* **62**, 743–755.

Tipper E. T., Galy A. and Bickle M. J. (2006a) Riverine evidence for a fractionated reservoir of Ca and Mg on the continents: implications for the oceanic Ca cycle. *Earth Planet. Sci. Lett.* **247**, 267–279. doi:10.1016/j.epsl.2006.04.033.

Tipper E. T., Galy A., Gaillardet J., Bickle M. J., Elderfield H. and Carder E. A. (2006b) The Mg isotope budget of the modern ocean: constraints from riverine Mg isotope ratios. *Earth Planet. Sci. Lett.* **250**, 241–253. doi:10.1016/j.epsl.2006.07.037.

Tipper E. T., Bickle M. J., Galy A., West A. J., Pomiès C. and Chapman H. J. (2006c) The short term climatic sensitivity of carbonate and silicate weathering fluxes: insight from seasonal variations in river chemistry. *Geochim. Cosmochim. Acta* **70**, 2737–2754. doi:10.1016/j.gca.2006.03.005.

Tucker C. J. (1979) Red and photographic infrared linear combinations for monitoring vegetation. *Remote Sens. Environ.* **8**, 127–150.

Walker J. C. G., Hays P. B. and Kasting J. F. (1981) A negative feedback mechanism for the long-term stabilization of Earth's surface temperature. *J. Geophys. Res.* **86**, 9776–9782.

West A. J., Galy A. and Bickle M. (2005) Tectonic and climatic controls on silicate weathering. *Earth Planet. Sci. Lett.* **235**, 211–228.

Wiegand B. A., Chadwick O. A., Vitousek P. M. and Wooden J. L. (2005) Ca cycling and isotopic fluxes in forested ecosystems in Hawaii. *Geophys. Res. Lett.* **32**, L11404.

Wieser M. E., Buhl D., Bouman C. and Schwieters J. (2004) High precision calcium isotope ratio measurements using a magnetic sector multiple collector inductively coupled plasma mass spectrometer. *J. Anal. Atom. Spectrom.* **19**, 844–851. doi:10.1039/b403339f.

Young E. and Galy A. (2004) The isotope geochemistry and cosmochemistry of Mg. *Rev. Min. Geochem.* **55**, 197–230.

Young E., Galy A. and Nagahara H. (2002) Kinetic and equilibrium mass-dependent isotope fractionation laws in nature and their geochemical and cosmochemical significance. *Geochim. Cosmochim. Acta* **66**, 1095–1104.

Zhu P. and Macdougall J. D. (1998) Calcium isotopes in the marine environment and the oceanic calcium cycle. *Geochim. Cosmochim. Acta* **62**, 1691–1698.

Associate editor: Clark M. Johnson